Shifts in organic matter character and microbial community dynamics from glacier headwaters to downstream rivers in the Canadian Rocky Mountains

by

Hayley Drapeau

A thesis submitted in partial fulfillment of the requirements for the degree of

Master of Science in the Department of Biological Sciences and Earth and Atmospheric Sciences

ABSTRACT

Climate change is causing mountain glacial systems to warm rapidly, leading to increased water fluxes from these catchments and concomitant export of glacially-derived sediment and organic matter (OM). Glacial OM represents an aged, but potentially bioavailable carbon pool that is compositionally distinct from OM found in non-glacially sourced waters. Despite this, the composition of riverine OM from glacial headwaters to downstream reaches and its role in structuring microbial communities has yet to be characterized in the Canadian Rockies. Over three summers (2019-2021) samples were collected from four glacially-fed rivers within Banff and Jasper National Parks. Samples were collected before, during and after glacial icemelt along a transect ranging 0 – 100 km downstream of glacial termini. Organic carbon (OC) isotopes (Δ^{14}C-OC, δ^{13}C-OC) were used to assess OM age and source, dissolved OM absorbance and fluorescence were used to assess OM character. Microbial community composition was assessed utilizing 16S rRNA gene sequencing. From headwater to rivers OM transitioned from being aged and protein-like with an apparent microbial source to being relatively younger, humic-like and sourced from plants and benthic algae. This transition was likely driven by changing catchment characteristics with movement downstream, and the presence of more developed soils. Total nitrogen, deuterium excess (correlated with glacial ice contribution), water temperature and protein-like DOM were significant in explaining microbial community structure, although only to a small extent (14%). This finding paired with the identification of a core community that made up large fraction of relative abundance at each site, indicating mass effects as driving a fraction of microbial community composition within these streams. Research into key taxa at sites near glaciers identified taxa that likely harbour adaptations to cold temperatures, nutrient poor conditions and chemolithoautotrophic metabolisms. This could indicate that glacially

exported microbes can seed proglacial stream communities. Together these findings suggest that both OC cycling and microbial community structure in glacier-fed streams in the Rockies will be impacted by glacial retreat, with unknown ecosystem impacts.

PREFACE

This thesis is an original work by Hayley Drapeau. The research is part of a collaboration between Dr. Suzanne Tank, Dr. Maya Bhatia, and Dr. Vince St Louis at the University of Alberta. I was responsible for the sample collection, lab and data analysis, and manuscript creation. Site selection and sample collection was completed with the help of Dr. Vince St. Louis and Jessica Serbu. Lab and data analysis was completed with the help of Maria Cavaco.

This thesis has three chapters: Chapter 1 is a general introduction of background concepts pertaining to the study, Chapter 2 is the chapter intended for publication, and Chapter 3 provides a summary of findings and recommendations for future research.

Chapter 2

Drapeau, H., Tank, S., Cavaco, M., Serbu., J, St. Louis V., and Bhatia, M. Shifts in organic matter character and microbial community dynamics from glacier headwaters to downstream rivers in the Canadian Rockies

ACKNOWLEDGMENTS

This thesis work would not be possible without help from mentors, collaborators, funding partners and many field assistants. I would like to thank, Dr. Maya Bhatia and Dr. Suzanne Tank for their support and guidance throughout my degree, you were both amazing mentors. Thank you to my collaborators Maria Cavaco, Jessica Serbu and Dr. Vince St. Louis. Processing and analysis of the microbial data would not have been possible without the assistance of Maria Cavaco. Dr. Vince St. Louis and Jessica Serbu assisted in study design, site selection and sample collection. I would also like to acknowledge the Alberta Conservation Association, Canadian Mountain Network and Alberta Innovates for helping fund this project. Finally, a very big thank you to everyone who assisted in field sampling: Lakoda Thomas, Samuel Metacat-Yah, Rory Burford, Sydney Enns, Janelle Flett, Charvanaa Dhoonmoon, Patrick White, Jill Lightbown, Craig Emmerson, Jaedyn Smith, Nora Alsafi, Leanne Drapeau and Jean-Louis Drapeau. With a special thank you to Lakoda Thomas and Rory Burford, I don't think I would have gotten through the 2021 field season without both of your friendship.

I would also like to thank all my peers in the Bhatia Lab and the Tank Lab for all your advice and support through the years. Special thanks to Jen Spence for all your help with analysing the microbial data, and Charvanaa Dhoonmoon for your assistance with the TOC and PARAFAC analysis. Thank you to Jaedyn Smith, Marina Taskovick, Nora Alsafi, Jillian Lightbown for your friendship, all the talks and laughs helped keep me sane through this degree. A very big thank you to my partner Patrick for your patience, encouragement, and support. Lastly, but certainly not least, thank you to my family, especially my sister Amy who loved the water and who continues to inspire me every day.

TABLE OF CONTENTS

LIST OF TABLES

LIST OF FIGURES

Chapter 1: General Introduction

1.1 Importance of glaciers to headwater stream environments

Alpine ice fields and glaciers are retreating at unprecedented rates worldwide (Zemp et al., 2015,Gardner et al., 2013). In western Canada, glacial coverage decreased by 31% from 2001 to 2010 (Zemp et al., 2015) and it is predicted that glaciers in this region will decrease by a further 70% by the year 2100 (Clarke et al., 2015). The loss of glaciers both globally and regionally will result in many ecosystem-scale effects (Milner et al., 2017), particularly with regards to freshwater availability (Anderson & Radić, 2020; Moore et al., 2009), food-web structure (Hotaling et al., 2017), and carbon cycling (Hood et al., 2015). Globally, terrestrial ice masses (glaciers, ice caps, ice sheets) are estimated to hold ~70% of the world's freshwater. Annually, as these ice masses melt in the summer, freshwater is released to downstream environments (streams, lakes, and oceans). In fluvial environments, seasonal contributions of glacial meltwater can impact stream hydrology, with glacially-fed streams augmenting summer discharge relative to snowmelt-fed stream systems (Moore et al., 2009, Milner et al., 2017). As glaciers retreat, meltwater contributions from glaciers will increase before an eventual decline, resulting in a shift in hydrological regime from glacial icemelt controlled (i.e., a glacial regime) to precipitation-controlled (nival regime) (Pradhananga & Pomeroy, 2022). In Alberta this shift is projected to result in decreased summer water availability, potentially impacting up to one million Albertans (Anderson & Radić, 2020).

Streams and rivers draining melting glaciers can transport glacial-origin organic matter (OM) to downstream aquatic ecosystems, and this transport has the potential to increase with climate-driven melt. By 2050, it is estimated that globally, melting glaciers will have exported 78 Tg of particulate OC (POC, OC > 0.7 μm) and 48 Tg of dissolved OC (DOC, OC < 0.45 μm) to headwater environments, with 56% of the DOC projected to originate from alpine systems relative to the polar ice sheets (Hood et al., 2015). Despite the low concentrations of OC (POC: 0.01-2.09 mg L^{-1} and DOC: 0.06 – 2.68 mg L^{-1} (Zhang et al., 2018)) that are typical of glacial systems, the contribution of glacial OC to headwaters may still have disproportionate ecosystem impacts due to its novel character (Hood et al., 2009; Singer et al., 2012). Over the last decade, studies have found that glacially-exported dissolved OM (DOM) is compositionally unique compared to the receiving environment and, by comparison, highly bioavailable to downstream

heterotopic microbial communities, leading to increased stream microbial productivity (Hood et al., 2009; Singer et al., 2012). Relative to glacially-exported DOC, less attention has been paid to glacially-exported POC, even though POC export with glacial melt is predicted to be substantial (Hood et al. 2015). Glacially-derived POC has previously been found to be sourced from subglacial petrogenic sources (Hood et al., 2020) or supraglacial microbial mats (Stevens et al., 2022). The majority of riverine ecosystems are heterotopic systems, with stream OC consumed and respired by microbial communities (Bernhardt et al., 2022) that can form the base of the food web (Roach, 2013). Since riverine OC character can drive microbial community structure (Jones et al., 2009; Judd et al., 2006; Muscarella et al., 2019), changes in glacially-exported OC may also impact microbial community composition in receiving fluvial networks, which could in turn, impact regional-scale biogeochemical cycles (Graham et al., 2016) and food web dynamics (Fellman et al., 2010).

1.2 Carbon pools in riverine environments

By definition, OM represents the combined mass of all elements in organic material (e.g., C, H, N, O) whereas OC refers specifically to the C fraction of the organic molecule (Nelson & Sommers, 1996).There are many ways that OM composition can be quantified, with bulk characteristics of the dissolved pool commonly determined through absorbance and fluorescence properties of DOM. DOM represents a heterogenous mix of dissolved organic compounds, and a fraction of these compounds can absorb light from different wavelengths (chromophoric DOM; CDOM), while a fraction of CDOM is able to fluoresce (fluorescent DOM; fDOM). Assessment of DOM absorbance and fluorescence properties have been utilized extensively to determine general OM characteristics (Helms et al., 2008; Huguet et al., 2008; McKnight et al., 2001a; Ohno, 2002; Weishaar et al., 2003). For example, absorbance-based metrics can be used to assess whether the bulk DOM pool is largely comprised of high or low molecular weight compounds (Helms et al., 2008), or displays a high degree of aromaticity (Weishaar et al., 2003). In tandem, measurements of fluorescence and subsequent statistical analyses can identify sub-components of the bulk DOM pool that display protein-like or humic-like fluorescent characteristics (Coble, 1996; Li & Hur, 2017). DOM that displays high protein-like fluorescence is thought to contain amino acid compounds (either free or in proteins) and is often associated with high lability (rapid consumption by microbes) (Fellman et al., 2010). In contrast, humic-like

fluorescence indicates the presence of compounds with high aromaticity (e.g., lignin, tannins), likely originally sourced from plant materials. In general, a high proportion of humic-like fluorescence often signifies a bulk DOM pool that is less labile than one that is more strongly dominated by protein-like DOM (Fellman et al., 2010).

To gain further insight into other important OC characteristics, like source and age, analysis of stable (^{12}C and ^{13}C) and radioactive (^{14}C) isotopes are often employed. Stable isotope ratios can be used to determine OM source because different environmental processes alter the rate of uptake of ^{12}C over ^{13}C resulting in an isotopic fractionation. This is typically expressed in a delta notation which indicates the ratio of the heavy isotope to the light isotope relative to a standard. For example, photosynthesis will preferentially uptake lighter carbon (^{12}C) (Peterson & Fry, 1987), resulting in isotopically light (depleted in ^{12}C) OM relative to the atmospheric CO_2 source. This depletion is relatively predictable in terrestrial environments, resulting in a typical $\delta^{13}C$-OC signature of -26 to -28‰ (Peterson & Fry, 1987). In aquatic environments, isotopic depletion is typically less pronounced in benthic than pelagic environments, because boundary layer-enabled CO_2 depletion inhibits fractionation (Hecky & Hesslein, 1995). In contrast, chemosynthetic metabolism such as methanogenesis and sulfur oxidation can cause large depletion in the $\delta^{13}C$-OC signature (Blaser & Conrad, 2016; Rau & Hedges, 1979; Ruby et al., 1987). OC age can be assessed using ^{14}C because the atmospheric ^{14}C incorporated into tissue during contemporary plant photosynthesis will begin to decay in accordance with the half-life of radiocarbon (5700 ± 30 yr) upon organismal death and the cessation of active CO_2 uptake (Bowman, 1990). By comparing the amount of ^{14}C relative to ^{12}C an age estimate of how long ago the original OC source was fixed can be obtained, up to ~50 000 years, when ^{14}C is no longer measurable. When combined, $\delta^{13}C$-OC and $\Delta^{14}C$-OC isotopic signatures can be useful for identifying mixtures of potential OC sources present in the environment (Raymond & Bauer, 2001).

1.3 The influence of stream hydrology on OC pools

The relative abundance of different sources of OM within a stream's bulk OM pool has clear ecological and biogeochemical implications. While some OM is produced within the stream itself, other sources are externally produced, and must therefore be transported to headwaters and downstream systems via hydrologic flowpaths. Because flowpaths can vary annually with

changing seasons, we must also consider the influence of stream hydrology and shifting water sources on OC pools. In alpine regions, summer stream inputs are sourced from either snowmelt or glacier icemelt depending on glacial extent (Smith et al., 2001). Rocky Mountain glacial contributions are highly seasonal, controlled by the onset of snowmelt in the spring, icemelt in the summer and cessation of glacial icemelt in the fall (Arendt, 2015). Typically in warm-based glaciers (i.e. the typical thermal regime for non-polar alpine glaciers) snowmelt is first routed from the glacier surface, via crevasses and moulins, to the base, joining a distributed drainage network consisting of a series of linked cavities along the ice-bed interface (Nienow et al., 1998; Paterson, 1994) Thus, the delivery of early season glacial meltwater to streams is dominated by contributions of subglacial meltwater draining this distributed network, marked by high water residence and rock:water interaction times with the underlying glacial till, sediment and bedrock (Nienow et al., 1998). As summer progresses, alpine glaciers experience increased surface melt which can create both ice marginal streams (i.e., channels located between lateral margins and the glacier with no contact with the glacier bed) and/or efficient subglacial drainage networks with surface meltwater joining a channelized drainage system at the ice-bed interface, which facilitates rapid water transport. As a result of the high fluxes, meltwater routed through the ice marginal or channelized subglacial drainage system typically has limited sustained rock:water interaction, leading to lower DOC and ionic concentrations (Kellerman et al., 2020; Tranter et al., 2002). However, these high meltwater fluxes can still mobilize large amounts of fine sediment via the ice-marginal and channelized drainage networks, leading to higher POC fluxes (Orwin et al., 2010).

Near the glacial termini, headwater streams are dominated by glacial meltwater sources, which proportionally decrease further downstream as other water sources (e.g., groundwater, subsurface flow through developed soils) join the growing fluvial network (Smith et al., 2001). Contributions from the terrestrial catchment in Rocky Mountain alpine streams have also been found to be seasonally controlled by snowmelt with the onset of snowmelt leading to a concentrated, solute-rich pulse of water from shallow soils into stream systems due to a lack of flushing during winter months, and subsequent build-up of solutes in soils (Campbell et al., 1995). As the season progresses, water from precipitation continues to be routed through soils, but is more dilute than the original pulse (Campbell et al., 1995). Towards the end of the

summer, water entering streams can become concentrated again, due to increased water residence time in soils (Campbell et al., 1995).

1.4 Microbes and carbon cycling

It is particularly important to consider microbial community dynamics in riverine systems because riverine ecosystems are heterotopic in that they are sustained by OM inputs that are consumed and largely mineralized by heterotopic microorganisms (e.g., Cole et al., 2001; Singer et al., 2012) which can be transferred to higher trophic levels (e.g., Fellman et al., 2015). In glacially-fed streams contributions of glacier microbes entrained in glacial meltwater may seed downstream communities (Stevens et al., 2022; Wilhelm et al., 2013). Glacier microbes exist on all areas of the glacier and have been found to possess adaptations for life in this extreme environment, including adaptations to low nutrient conditions, low temperatures, and anoxic conditions (i.e., via chemosynthesis in sub-glacial environments) (Bourquin et al., 2022; Hotaling et al., 2017; Stibal et al., 2012b). Given the common hypothesis that microbial community structure is predominately determined based on environmental characteristics (the Baas Brecking hypothesis: "everything is everywhere but the environment selects"), it is expected that exported novel glacier microbes quickly dissipate from the community as they transit downstream (Bourquin et al., 2022) due to associated changes in environmental conditions that no longer favour their dominance. Supporting the Baas Brecking hypothesis, environmental drivers such as nutrients and light availability are frequently associated with microbial community composition (Bernhardt et al., 2022; Bourquin et al., 2022; Elser et al., 2020; Milner et al., 2017). In particular, OM characteristics can shape microbial community composition, through the ability of certain heterotopic microbes to specialize on different components of the broader OM pool (Judd et al., 2006; Muscarella et al., 2019). This may allow for certain microbial species to dominate microbial communities at times when their preferred substrates are present at high amounts and diminish when these substrates are in low supply (Judd et al., 2006). In turn, microbial communities can alter OM character through the production, consumption and modification of OM components (Kujawinski, 2011). Thus, OM character and microbial communities are linked, with changes in character potentially resulting in microbial community changes and vice versa.

1.5 Study Region

My thesis focuses on glacially-fed streams and rivers sourced from outlet glaciers in the Canadian Rocky Mountains, specifically the Colombia and Wapta icefields. The Canadian Rocky Mountains were formed over 100 mya (Chen et al., 2019), with the range beginning in British Colombia and spanning a large proportion of the Alberta-British Colombia border. The Rockies have gone through several periods of glaciation and deglaciation since their formation, with current glaciers and ice fields formed throughout cold periods during the Holocene (over the last 11,700 years). Currently, these ice masses are retreating from their most recent maximum extent during the Little Ice Age (~1840 CE; common era) (Luckman, 2017). As a result of anthropogenic-driven climate change, meltwater contributions into glacially-fed streams in the Rockies are continuing to increase (Pradhananga & Pomeroy, 2022) but are projected to begin to decline between the present day and 2040 (Clarke et al., 2015). Our study rivers form major watersheds within Alberta (the Athabasca, North Saskatchewan, and South Saskatchewan Rivers) that eventually drain into the Arctic Ocean (Athabasca River) and Hudson Bay (North and South Saskatchewan Rivers). The loss of glacial meltwater contributions into these rivers will undoubtedly have downstream impacts as glacier-fed streams in this region provide essential services, including hydropower, municipal water supply and irrigation (Anderson & Radić, 2020), alongside other ecosystem functions such as biogeochemical cycling, biodiversity, and structuring food webs (Milner et al., 2017).

1.6 Research goals and objectives

Recent findings in other mountain glacial systems (e.g., the Alps, Alaska) show that melting glaciers export labile OM downstream (Hood et al., 2009; Singer et al., 2012) that can impact microbial community productivity (Singer et al., 2012). The purpose of this thesis is to investigate whether the presence of glaciers affects OM composition in glacially-fed alpine streams, and whether this, in turn, impacts microbial community structure. Using samples collected between 2019 – 2021, I explored this question over varying distance ranges from the glacial headwater source and throughout the meltwater season (from spring thaw to fall freeze-up) to assess how OC pools, microbial communities and their relationship evolved with increased distance from glaciers and across seasons. My exploration of these coupled OC-microbial community dynamics will allow us to better predict how microbial communities and

OC pools will change with glacial loss in glacially-fed alpine streams. The specific objectives of this thesis were to:

1. Investigate spatial and temporal variation in stream OC pool age, source, and character across different hydrological periods in four Rocky Mountain rivers with a distance ranging from 0-100km downstream from glacial termini.
2. Characterize microbial community composition from glacial headwaters to downstream rivers; and
3. Identify environmental drivers of microbial community structure, with a particular focus on OM character.

1.7 Significance

Both stream OC and microbial communities exhibit seasonal variation associated with changes in water flow paths and stream characteristics such as temperature (Crump et al., 2003; Kellerman et al., 2021). This study is the first, to our knowledge, to assess seasonal changes in glacial-fed stream microbial communities and OC pools in Rocky Mountain streams from their headwaters to over 100 km downstream. As climate change continues, headwater streams will become less glacially influenced. Through assessment of OM characteristics, spanning a continuum of high glacial influence to relatively lower glacial influence, this study will allow us to better predict the coupled microbial-OM response to glacial retreat in this region. Additionally, Rocky Mountain glacier OM dynamics has been understudied relative to other regions, such as the Alps (e.g., Singer et al., 2012), Greenland (e.g., Bhatia et al., 2013; Kellerman et al., 2021), Alaska (e.g., Stubbins et al., 2012), Tibetan plateau (e.g Zhou et al., 2019), and alpine proglacial microbial community composition is also generally critically understudied (Bourquin et al., 2022). Thus, this research will help fill a gap in glacial impacts on carbon cycling globally and on proglacial microbial community structure.

Chapter 2: Shifts in organic matter character and microbial community dynamics from glacier headwaters to downstream rivers in the Canadian Rocky Mountains

2.1 Introduction

Anthropogenic climate change is causing glaciers to retreat at unprecedented rates (Zemp et al., 2015). This rapid glacial retreat has the potential to impact downstream hydrology (Clarke et al., 2015), carbon cycling (Hood et al., 2015; Hood et al., 2020) and microbial community dynamics (Bourquin et al., 2022; Hotaling et al., 2017), as source water contributions to headwater streams undergo fundamental change. In the Canadian Rocky Mountains glacial meltwater contributions to downstream rivers is presently increasing but is projected to decline by 2040 (Clarke et al., 2015; Pradhananga & Pomeroy, 2022). The eventual disappearance of glacial meltwater additions to glacially-fed rivers is predicted to lead to decreased summer flows and water availability, impacting up to 1 million Albertans (Anderson & Radić, 2020).

Changing contributions of glacial meltwater to headwater streams could disrupt downstream riverine carbon dynamics, because glaciers provide, and internally cycle, unique sources of OC (Hood et al., 2015; Musilova et al., 2017; Wadham et al., 2019). As glaciers melt, englacial and marginal channels form which can cause meltwater to be routed on top of, through, and/or underneath, glaciers (Nienow et al., 1998). At the beginning of the melt season, water is typically sourced from snowmelt which is inefficiently routed through a distributed hydrological network at the ice-bed interface or along the ice margin, and is characterized by high rock:water contact times (Arendt, 2015). As the melt season progresses an efficient subglacial network forms facilitating rapid transit through the subglacial environment (Arendt, 2015) or routing of water laterally via marginal streams. This meltwater is then exported into headwater streams where it provides a large seasonal control on stream hydrology via augmentation of summer discharge (Campbell et al., 1995). This contribution of glacially-sourced water to headwater streams enables movement of novel glacially-sourced OC (e.g., from over-ridden vegetation (Bhatia et al., 2010), anthropogenic aerosols (Stubbins et al., 2012), and microbial communities (Stibal et al., 2012)) to downstream systems (Dubnick et al., 2010). Previous studies have shown that glacially-derived dissolved OM (DOM) is aged (Bhatia et al., 2013; Hood et al., 2009; Stubbins et al., 2012), exhibits protein-like fluorescence (Dubnick et al., 2010; Kellerman et al., 2020), and can serve as a labile substrate for downstream microorganisms (Hood et al., 2009;

Singer et al., 2012). In contrast, glacially-derived particulate OM (POM, and its OC subset; POC) has been less well studied, but is thought to be derived largely from comminuted rock and sediment, and to persist within rivers (i.e., is a poor substrate for downstream microbial consumption) (Hood et al., 2020). During transit through fluvial networks, glacially-exported OM mixes with more traditional terrestrially-derived OM sources, which typically have humic-like fluorescent signatures (McKnight et al., 2001b), are relatively younger (Raymond & Bauer, 2001), and have generally been shown to be less accessible for microbial consumption (D'Andrilli et al., 2015).

River ecosystems are overwhelmingly heterotrophic, with food webs sustained by microbial consumption and mineralization of OM inputs (Bernhardt et al., 2022). OM characteristics have been found to be important drivers of microbial community structure (Judd et al., 2006) alongside other environmental characteristics such as light, river flow regimes (Bernhardt et al., 2022; Milner et al., 2017), temperature, and nutrient availability (Elser et al., 2020). Thus, the increase and eventual decline of glacial meltwater inputs to fluvial networks, with their associated entrained glacial OM, may impact microbial community structure. In addition, headwater communities could also shift as a result of the direct loss of glacially-sourced microbial members (Wilhelm et al., 2013) as glaciers have been found to host unique microbial taxa both in the supraglacial and subglacial environments (Bourquin et al., 2022; Hotaling et al., 2017; Stibal et al., 2012). These taxa are often uniquely adapted to glacial conditions, such as seasonally-fluctuating and overall low nutrient concentrations, cold temperatures, and the presence of reduced chemical species in low oxygen subglacial environments, which can lead to chemosynthetic metabolisms (Bourquin et al., 2022; Hotaling et al., 2017). Recent work on European, Greenlandic and North American glaciers found that glacial meltwater contained an average of 10^4 microbial cells mL^{-1} sourced from the supraglacial environment, highlighting the potential of supraglacial microbes to seed downstream communities (Stevens et al., 2022). Overall, if changes in glacial loss drive changes in microbial community composition, this could lead to a loss of unique metabolic pathways (Bourquin et al., 2022), changes in respiratory efflux of CO_2 (e.g Singer et al., 2012), and food web perturbations, given that OM incorporated into microbial biomass is assimilated by higher trophic level organisms (e.g Fellman et al., 2015) .

In this study, we pair measurements of stream OM and microbial community composition along transects from glacial headwaters to downstream rivers across different hydrological periods. We undertake this work in glacially-fed fluvial networks draining eastward from the Canadian Rocky Mountains, to assess how glacial loss will impact stream microbial diversity and carbon cycling in this region. Our objectives were three-fold: first, to investigate spatial and temporal variation in stream OM age, source, and character across different hydrological periods in three Rocky Mountain rivers with a distance ranging from 0-100km downstream from glacial termini; second, to characterize microbial community composition from glacial headwaters to downstream rivers; and finally, to identify environmental drivers of variation in microbial community structure, with a particular focus on OM character. This work will increase our understanding of glacial carbon cycling globally as this region is relatively understudied compared to other glacierized regions (Greenland (e.g Bhatia et al., 2013; Kellerman et al., 2021), Alaska (e.g Stubbins et al., 2012), and the Tibetan plateau (e.g Zhou et al., 2019)). In addition, this work will critically expand knowledge on cryosphere microbiomes, as mountain glacial systems are particularly poorly studied, despite the fact that these microbiomes are thought to host functionally unique microbial taxa particularly vulnerable to climate change (Bourquin et al., 2022).

2.2 Methods

2.2.1 Site Description

Samples were collected from the Athabasca-Sunwapta, North Saskatchewan (NSR) and Bow Rivers located within Banff and Jasper National Parks in the Canadian Rocky Mountains. Each of these rivers are sourced from glacial headwaters with the Athabasca-Sunwapta and NSR receiving inputs predominately from the Colombia Icefield, and the Bow River receiving inputs from the Wapta Icefield. At 325 km^2, the Colombia Icefield is the largest icefield in the Canadian Rockies, while the Wapta Icefield is only slightly smaller at 221 km^2. Similar to other glaciers in the Rocky Mountains, both the Colombia and Wapta icefields are rapidly retreating and are projected to be reduced by 80-100% of their 2005 area by 2100 (Clarke et al., 2015). Due to the increasing rates of glacier loss, glacier meltwater inputs to rivers are currently increasing (Pradhananga & Pomeroy, 2022), and are projected to peak at some point before 2040 (Clarke et al., 2015). This change is projected to have impacts on stream hydrology (Pradhananga &

Pomeroy, 2022), aquifer recharge (Castellazzi et al., 2019), biodiversity (Hotaling et al., 2019) and stream biogeochemistry (Milner et al., 2017).

Along each river we chose three to four sampling sites at which we examined how stream OM and microbial characteristics evolved with increasing distance from glacial input. Samples were collected over a three-year study period (2019-2021) (Table A.1), with sample collection occurring approximately monthly during the flowing water season (see below). The total distance sampled ranged from glacial headwaters (0 km downstream of glacial inflow) to 100 km downstream of glacial termini. For certain analyses, sites were binned into four distance ranges: headwater (0 km downstream), near (3-7 km downstream), mid (18-35 km downstream) and far (40-100 km downstream). Sites were restricted to locations within Banff and Jasper National Parks to enable a comparison of study sites that were minimally impacted by direct anthropogenic landscape disturbance.

Each of the sample sites were visited every three to four weeks throughout the months of May to October during 2019, 2020, and 2021. Samples were also collected at select sites in December 2019 and January 2021. This sampling design enabled us to cover the three main hydrological stages in a glacially-sourced river: prior to the seasonal glacial icemelt (pre-melt), the glacial melt period (melt), and the post-glacial icemelt period (post-melt). We defined the pre-melt stage as the period when monthly average stream discharge at the Athabasca glacier headwater was low (< 1 m^3 s^{-1}); a likely indication that glacial meltwater channels were not yet established (Arendt., 2015) (Fig. 2.1). The glacial melt period was defined as the period when monthly average discharge was high (> 2.5 m^3 s^{-1}; discharge typically peaked during July-August) (Fig. 2.1); at this time glacial meltwater channels were likely well-established, with melting glacier ice contributing substantially to headwater stream flow. Finally, the post-melt period was characterized by low average monthly discharge at the glacier headwater (< 1 m^3 s^{-1}; typically October and onwards); likely indicating closed glacial channels and cessation of icemelt input (Figure 2.1). Hydrological periods were determined through visual assessment of stream discharge hydrographs at the Athabasca glacier (station ID: 07AA007) collected by Environment and Climate Change Canada (ECCC) (ECCC, 2022).

2.2.2 Field Sampling and Field and Laboratory Processing

At each site samples were collected for: DOM absorbance and fluorescence, DOC concentration, POC concentration, particulate, and dissolved OC isotopes (δ^{13}C-DOC, δ^{13}C-POC, Δ^{14}C-DOC, Δ^{14}C-POC), and 16S rRNA gene sequencing for microbial community composition analysis. To further assess water source and controls on microbial diversity in our analyses, we also sampled for water isotopes (δ^{18}O-H_2O, δ^{2}H-H_2O), nutrients (ammonia (NH_4), nitrate and nitrite (NO_3+NO_2), total dissolved nitrogen (TDN), total nitrogen (TN), soluble reactive phosphorous (SRP), total phosphorous (TP), and dissolved silica (dSi)), major anions and cations (Mg, Cl, Na, SO_4, Ca, K), temperature, and specific conductance. All sample bottles were soaked overnight in a dilute acid bath (1.2 mol L^{-1} trace metal grade HCl), rinsed at least 3 times with 18.2 MΩ MilliQ water, and, before collection at the field site, rinsed three times with sample water. Following the HCl soak and MilliQ water rinse, all glassware (bottles, EPA vials, and filtration apparatuses) were combusted at 560°C for a minimum of four hours, and high-density polycarbonate (HDPC) bottles for microbial analysis were autoclaved. Glass microfibre filter (grade GF/F, Whatman) membranes were combusted at 460°C for a minimum of four hours prior to use. High-density polyethylene (HDPE) bottles for ion collection were pre-washed with Citronex prior to the acid cleaning procedure.

Samples for DOM absorbance and fluorescence, DOC concentration and δ^{13}C-DOC were sub-sampled from a 250 mL amber glass collection bottle and filtered streamside through 0.45 μm PES filters (Fisherbrand Basix; pre-rinsed with 60 mL Milli-Q and 15 mL river water) into combusted 40 mL amber EPA vials. Nutrient samples were sub-sampled from a 500 mL HDPE collection bottle and filtered streamside using a pre-rinsed sterile plastic syringe and a pre-rinsed 0.45 μm cellulose acetate filter (Sartorius) into polypropylene collection bottles. Water isotope samples were filtered streamside using 0.45 μm PES filters into HDPE scintillation vials filled with no headspace. Major ions were sub-sampled from a 250 mL HDPE collection bottle into 20 mL scintillation vials using rubber-free syringes and a 0.45 μm PES filter. Water temperature and specific conductance were measured on-site using a YSI EXO sonde. Bulk water samples were collected for microbial 16S rRNA gene samples in HDPC bottles, radiocarbon in Teflon bottles, and POC and δ^{13}C-POC samples in 4L HDPE plastic bottles. All bulk water samples for water chemistry and OC were filtered within 24 hours of collection off site. Samples for 16S rRNA gene sequencing were generally filtered within 4-12 hours of collection, apart from the

Bow River samples that were filtered after 24 hours of collection. Thus, to minimize the effects of this inconsistency in sample processing, particularly with regards to molecular sequencing, the Bow River samples were excluded from our microbial analysis but retained in the hydrochemical and carbon analyses.

Bulk water collected for 16S rRNA gene sequencing were processed using a 0.22 μm sterivex (MilliporeSigma) filter and a peristaltic pump operated at 50-60 mL min^{-1} to minimize cell breakage. Dissolved radiocarbon samples were filtered through a 0.7 μm GF/F filter using a glass filter tower, collected into 1L amber glass bottles, and acidified to pH 2 using HPLC grade H_3PO_4. Material retained on the 0.7 μm GF/F filter was used for Δ^{14}C-POC analysis. Samples for POC concentration and δ^{13}C-POC were collected on 0.7 μm GF/F filters using plastic filter towers. Samples for DOC concentration and δ^{13}C-DOC were acidified to pH 2 using trace metal grade HCl and cation samples were acidified to pH 2 using trace metal grade HNO_3. Samples for DOC concentration, δ^{13}C-DOC, Δ^{14}C-DOC, DOM absorbance and fluorescence, ions, TDN, TDP and dSi were stored at 4°C; samples for NH_4, NO_3+NO_2, δ^{13}C-POC, Δ^{14}C-POC were stored at -20°C, and sterivex filters were flash frozen in a liquid nitrogen dry shipper and upon return the laboratory stored at -80°C until analysis.

2.2.3 Laboratory analyses

2.2.3.1 DOM absorbance and fluorescence, DOC, POC and OC isotopes

DOM absorbance and fluorescence were analysed using a HORBIA Scientific Aqualog with a 1cm path length quartz cuvette. Absorbance scans were collected over a 240-800 nm wavelength range in 1nm increments with a 0.5 second integration time. Excitation emission matrices (EEMs) were constructed over a 230-500 nm excitation wavelength range with an increment of 5 nm and a 5 second integration time, with an emission coverage increment of 2.33nm with a 230-500 nm emission wavelength range.

DOC samples were analyzed using a Shimadzu Total Organic Carbon analyzer. Samples with less than 1 mg L^{-1} DOC were analyzed on a Shimadzu TOC-V equipped with a high sensitivity catalyst, using a 2 mL injection and five-minute sparge time. Samples estimated (from absorbance) to have more than 1 mg L^{-1} DOC were analyzed using a Shimadzu TOC-L fitted with a regular sensitivity catalyst, using a 150 μL injection and five-minute sparge time. For analyses on the TOC-V, a five-point (0-1 mg L^{-1}) or six-point (0-0.5 mg L^{-1}) calibration curve

($R^2 > 0.98$) was created daily using dilution from a 5 mg L^{-1} stock solution (SCP Science). For analyses on the TOC-L, a five-point (0-1 mg L^{-1} or 0-2 mg L^{-1}) calibration curve ($R^2 > 0.98$) was created through dilution of either 5 mg L^{-1} stock solution (SCP Science) or a 10 mg L^{-1} stock solution (SCP Science). Reference waters were created using dilution of a 5 mg L^{-1} stock solution (SCP Science) or from a 1 mgC L^{-1} caffeine solution. Reference waters and MilliQ blanks were run every ten samples and were within 10% of accepted values. Samples were blank corrected via the subtraction of mean blank concentrations of MilliQ samples run prior to sample groups to account for instrument drift.

POC, δ^{13}C-POC and Δ^{14}C-POC samples were subjected to a heated acid fumigation following procedures outlined in Whiteside et al. (2011). Briefly, this involved heating the filters at 60°C for 24 hours in a desiccator with 20 mL of concentrated HCl, then neutralizing the filters at room temperature for 24 hours in a desiccator with NaOH pellets. Samples for POC concentration and δ^{13}C-POC were packaged into tin capsules before being measured using an Elementar VarioEL Cube Elemental Analyser a DeltaPlus Advantage isotope ratio mass spectrometer with a ConFlo III interface (δ^{13}C-POC only) at the Jan Veizer Stable Isotope Laboratory (Ottawa, ON, Canada). δ^{13}C-DOC samples were analysed using the wet oxidation method on an OI Analytical Aurora model 1030 wet TOC analyser connected to an Isotope Ratio Mass Spectrometer (IRMS) at the Jan Veizer Stable Isotope Laboratory. Δ^{14}C-POC samples were processed via organic combustion and Δ^{14}C-DOC samples were processed using UV-oxidation, prior to graphitization and accelerator mass spectrometry analysis at the National Ocean Sciences Accelerator Mass Spectrometry laboratory (NOSAMS; WHOI, Woods Hole, MA, USA; Batch numbers = 67580, 67380, 67069, 66828).

2.2.3.2 Hydrochemical Samples

Nutrients (NH_4, NO_3+NO_2, TDN, TN, TP, dSi, SRP) and ion (Mg, Cl, Na, SO_4, Ca, K) samples were analysed at the CALA (Canadian Association for Laboratory Accreditation) accredited Biogeochemical Analytical Service Laboratory at the University of Alberta, Edmonton, AB, Canada). Nutrient samples were analyzed using flow injection analysis on a Lachat QuikChem 8500 FIA automated ion analyzer and ions were analyzed via ion chromatography on a Dionex DX600 and Dionex ICS 2500 following standard operating procedures. Water isotopes (δ^{18}O-H_2O and δ^{2}H-H_2O) were analyzed using a Picarro L2130 isotope and gas concentration analyzer

calibrated using standard references obtained from ice core water (USGS46) and Lake Louise drinking water (USGS47) (United States Geological Survey). Reference waters and MilliQ were run every 20 samples and were within 20% of accepted values. Sample values were calculated from an average of three injections where the standard deviation of $\delta^{18}O\text{-}H_2O$ was less than 0.2 and the standard deviation for $\delta^{2}H\text{-}H_2O$ was less than 1; the first five injections were typically excluded due to memory effects. $\delta^{18}O\text{-}H_2O$ and $\delta^{2}H\text{-}H_2O$ were used to calculate deuterium excess (d) (Boral et al., 2019).

2.2.3.3 Lab and Bioinformatic Processing of Microbial Samples

Stream water DNA was extracted using a DNEasy PowerWater Sterivex kit (Qiagen) according to the manufacturer's instructions (Qiagan, 2019) with an amendment of a 1-hour 72°C incubation time, rather than 90°C for 5 minutes, to increase DNA yield. Extracted samples were amplified using the 515F (5'GTGYCAGCMGCCGCGGTAA'3) and 926R (5'CCGYCAATTYMTTTRAGTTT'3) primers targeting the V4-V5 hypervariable region of the 16S rRNA gene with the following protocol: 3 min initial denaturation at 98°C, 35 cycles of: 30 s denaturation, 30 s primer annealing at ~ 60°C and 30 s extension at 72°C; and finally, 10 mins of final extension at 72°C. Polymerase Chain Reaction (PCR) products were visualized on a 1.5% agarose gel and those samples showing product on the gel were subsequently purified using Nucleomag beads (ThermoFisher Scientific). Unique indices were then added to each sample using i7 and i5 adapters (Illumina) to construct the subsequent library. All amplicon and barcoded products from each respective year of sampling (2019, 2020, 2021) were verified on a 1.5% agarose gel and those that could be successfully visualized were then pooled (12.4 ng μL^{-1}, 20.17 ng μL^{-1}, 14.3 ng μL^{-1}). The final quality of each pool was determined on an Agilent 2100 Bioanalyzer at the Molecular Biology Service Unit (MBSU, Univ. of Alberta, Edmonton, AB, Canada) using a high sensitivity DNA assay prior to submitting the library for 16S rRNA gene sequencing. The final prepared 2-4 nM libraries, containing up to 50% PhiX Control v3 (Illumina, Canada Inc., NB, Canada) were sequenced on an Illumina MiSeq (Illumina Inc., CA, USA) using a 2 × 250 cycle MiSeq Reagent Kit v3 submitted at the Molecular Biological Services Unit (Univ. of Alberta) in 2019 and The Applied Genomics Core (Univ. of Alberta) in 2020 and 2021.

Sequence data was demultiplexed using MiSeq Reporter software (version 2.5.0.5) and Miseq Local Run Manager GenerateFastQ Analysis Module 3.0. The assembled data was then processed using the Quantitative Insights into Microbial Ecology (QIIME2) pipeline (Boylen et al., 2020, version 2021.11). Sequences were clustered into amplicon sequence variants (ASVs) with chimeric sequences, singletons and low abundance ASVs removed using DADA2 (Callahan et al., 2019). All representative sequences were classified with the SILVA taxonomic database, using the most recent release (version 138; Quast et al., 2013, Yilmaz et al., 2014). ASV sequences that were identified as eukaryotes or chloroplasts were removed. Samples were decontaminated by removing ASVs present in a sequenced field blank using the prevalence method (Karstens et al., 2019; Parada et al., 2016).

2.2.4 DOM absorbance and fluorescence calculations and PARAFAC analysis

EEMs were corrected for inner filter effects, Raman normalized, blank corrected and had Rayleigh and Raman scatter bands removed prior to parallel factor (PARAFAC) analysis (Murphy et al., 2013). PARAFAC analysis was performed in Matlab (Version 9.12.0) using the drEEM toolbox (Version 0.6.5) (Murphy et al., 2013). PARAFAC models of up to seven components were assessed and samples with high leverage were removed. A four-component model was validated using split-half analysis (Fig. A.1) and was ultimately selected based on a low sum of square error and visual confirmation that only random noise remained in the residuals. Absorbance scans were utilized to calculate specific UV absorbance at 254 nm ($SUVA_{254}$; a measure of DOM aromaticity) (Weishaar et al., 2003) and the spectral slope coefficient ($S_{275\text{-}295}$; a measure of DOM molecular weight) (Helms et al., 2008). Corrected fluorescence data were utilized to calculate the fluorescence index (FI) (McKnight et al., 2001a), humification index (HIX) and biological index (BIX) (Huguet et al., 2008). Further description of absorbance- and fluorescence-based metrics is provided in Table A.4.

2.2.5 Data Analysis and Visualization

2.2.5.1 Water Isotope Model

A three-component mixing model was constructed using d and $\delta^{18}O\text{-}H_2O$. The end-members employed in the model were glacial icemelt, snow, and summer precipitation, each of which were collected at the Athabasca glacier in 2011 (Table. A.2, Table. A.3)(Arendt, 2015).

Proportions of each end member represented in each sample were calculated using the following series of equations:

(1) $$f_{ice} + f_{snow} + f_{summer} = 1$$

(2) $$\delta^{18}O: f_{ice}\,\delta^{18}O_{ice} + f_{snow}\,\delta^{18}O_{snow} + f_{summer}\,\delta^{18}O_{summer} = \delta^{18}O_{sample}$$

(3) $$d: f_{ice}\,d_{ice} + f_{snow}\,d_{snow} + f_{summer}\,d_{summer} = d_{sample}$$

2.2.5.2 Organic matter

Three-way ANOVAs followed by Tukey's honest significant difference (HSD) post-hoc tests were performed to determine whether OC concentration, OM character, and OC isotopic composition varied across distance bins, hydrological periods, and years. Linear regressions were performed to assess the relationship between the glacial ice fraction and PARAFAC components, and the relationship between Δ^{14}C-DOC and PARAFAC components. To explore how OM parameters varied across hydrologic seasons and with distance downstream sample space a principal component analysis (PCA) was performed. Water source contributions were fitted onto the ordinated PCA as a passive variable.

2.2.5.3 Microbial analysis

To enable contrasts between sites most strongly influenced by glaciers (the headwater and near sites), and those further downstream, the mid distance range sites were excluded from statistical analysis of the microbial samples. Alpha diversity was calculated using the Shannon index (Hill, 1973) and beta diversity was assessed using non-parametric multi-dimensional scaling (NMDS) with a Bray Curtis distance matrix of Hellinger-transformed amplicon sequence variant (ASV) abundance data. Significant differences between clusters on the NMDS were assessed using permutational multivariate ANOVAs (perMANOVA). A backward step redundancy analysis (RDA) was also performed on Hellinger-transformed ASV abundance data and non-correlated normally scaled environmental parameters. Initially-considered environmental parameters in our RDA included temperature, pH, specific conductance, turbidity, DOC concentration and DOM composition (% humic-like, FI, BIX, HIX, peak A, peak B, peak C, peak M, peak T, $S_{275\text{-}295}$, $SUVA_{254}$), nutrients (TP, TDN, dSi), major ions (Cl, SO_4, Ca, K, Mg, Na), and metals (Al, Ba, Cr, Mn, Mo, Ni, Sr). An indicator species analysis (ISA) was performed on raw (non-transformed) ASV abundance data. Co-variation between indicator species and environmental

parameters (nutrients, cations, anions, OC, glacial melt input, discharge, water temperature, and specific conductance) was assessed using Spearman's rank correlation.

2.2.5.4 Software

All data was analyzed with the R programming language, using *vegan* (Oksanen, 2007), *stardom* (Pucher et al., 2019), *decontam* (Davis et al., 2018), *indicspecies* (Cáceres & Legendre, 2009), and base packages (R Core Team, 2022). Data visualization utilized the package *ggplot2* (Wickham H, 2016).

2.3 Results

2.3.1 Spatial and temporal variation in stream carbon pool characteristics

2.3.1.1 Spatial and temporal trends in water isotopes

Across all sampling years (2019-2021), d was higher at the headwater and near sites relative to mid and far sites; seasonally d was greater during melt and post-melt periods relative to pre-melt periods ($p < 0.001$) (Fig. A.4). Trends in modelled glacial icemelt mirrored trends in d (Fig. A.4, Table. A.5), with icemelt contributing up to 60% of streamflow during the pre-melt season at headwater sites, declining to 32% with movement downstream. $\delta^{18}O\text{-}H_2O$ became more enriched throughout the season and mirrored modelled contributions from summer precipitation. Specifically, summer precipitation comprised a greater proportion of stream water during post-melt periods, compared to melt and pre-melt, and during melt periods, compared to the pre-melt period ($p < 0.001$) (Fig. A.4, Table. A.6).

2.3.1.2 DOC concentration and DOM composition

Overall, DOC concentration ranged from 0.07 mg L^{-1} near glacier termini to 3 mg L^{-1} at downstream sites during the 2019 pre-melt period (Fig. 2.2a). Across all years, DOC concentrations closest to the glacier were universally low (0.09-0.76 mg L^{-1}) and increased downstream (e.g., the far sites had significantly higher DOC concentrations compared to the headwater, mid and near sites, and the mid sites had significantly higher concentrations than the near sites; $p < 0.001$) (Fig. 2.2a, Table. A.7). In addition, pre-melt season DOC concentrations were greater than during the melt season (2019 and 2021), and concentrations during 2019 were greater than observed 2020 and 2021 ($p < 0.01$) (Fig. 2.2a, Table. A.7). POC concentrations

ranged from 0.04 mg L^{-1} to 2.8 mg L^{-1} across all sites and dates, with concentrations significantly greater at the headwater sites than at the near sites, and in 2019 relative to 2021 (Fig. 2.2d, Table. A.8) ($p < 0.05$). POC concentrations did not differ significantly between headwater and mid or far sites; or between near and mid or far sites (Fig. 2.2d, Table. A.8). POC was typically the dominant component of the total OC (TOC) pool at headwater sites (POC: TOC = 0.32-0.89), and the proportion of POC in the TOC pool declined downstream (POC:TOC = 0.1- 0.52 at the furthest downstream site) (Fig. 2.2e).

From the suite of PARAFAC models considered, a four-component model was selected (Fig. A.1). Using the OpenFluor database (Murphy et al., 2014), components 1 (C1) and 2 (C2) were identified as humic-like components, component 3 (C3) was identified as a tryptophan-like (protein-like) component, and component 4 (C4) was identified as a tyrosine-like (protein-like) component (Table. A.2). The proportion of protein- (sum of C3 and C4) and humic- (sum of C1 and C2) like components varied across our distance bins, with the proportion of protein-like DOM decreasing with increasing distance downstream, and the proportion of humic-like components showing the inverse relationship ($p < 0.05$) (Fig. 2.2a-b, Table. A.9). Broadly speaking, in 2019 and 2021, the proportion of protein-like DOM increased while humic-like DOM decreased, from pre-melt to melt periods, this trend was most prominent at mid and far sites ($p = 0.04$) (Fig. 2.2a-b, Table. A.9). A relationship between the modelled proportion of water derived from glacial melt and DOM composition was evident, with the proportion of protein-like DOM being positively correlated with glacial icemelt fraction ($R^2_{adj} = 0.22$, $p < 0.001$) (Fig. 2.3).

2.3.1.3 Particulate and dissolved OC isotopes

δ^{13}C-DOC ranged from -35 to -20.2‰ (Fig. 2.4) across sites and was significantly more depleted during the pre-melt and melt season relative to post-melt season, and in 2020-2021 compared to 2019 (Table. A.10). δ^{13}C-POC ranged from -38.8 to -20.8‰ (Fig. 2.4) and across all sites was significantly more depleted during the pre-melt season ($p < 0.001$) and in 2019 ($p < 0.001$) (Fig., A.2, Table. A.11). Spatially, Δ^{14}C-DOC generally became more depleted with increasing proximity to glacier termini ($p=0.08$, Table. A.12) but exhibited high variability at the headwater site during the melt season (Fig. 2.5a). Stream Δ^{14}C-DOC also varied seasonally, generally becoming more depleted from pre-melt to post-melt ($p = 0.003$) (Fig. 2.5a, Table. A.12). In

addition, stream Δ^{14}C-DOC showed a modest negative correlation with protein-like DOM (R^2_{adj} = 0.15, p = 0.006) (Fig. 2.5b), with increasing depletion in Δ^{14}C-DOC as the percent contribution of protein-like DOM increased. Δ^{14}C-DOC ranged from -554‰ to +7‰ (n = 8) at the Athabasca glacier headwaters, -634‰ to +18‰ at near sites (n = 16), -404‰ to +27‰ at mid sites (n = 24) and increased to +71‰ when measured during the pre-melt season ~50km downstream from glacier terminus (n = 1) (Fig. 2.4). Similarly, Δ^{14}C-POC also exhibited a large range in values, from -550‰ to -108‰ (Fig. 2.4).

2.3.1.4 Principal component analysis

A principal component analysis exploring DOM composition across sites identified eight principal components with 64% of the observed variation being explained by the first two principal component axes. Principal component 1 (PC1) explained 48% of sample variance, and described a compositional range associated with fluorescence characteristics with humic-like PARAFAC components, DOC concentration and HIX (humification) loading positively on PC1, and protein-like PARAFAC components, BIX (biological origin), FI (microbial origin), and $S_{275-295}$ (declining molecular weight) loading negatively. Sites generally plotted along PC1 according to their distance range, with headwater and near sites more frequently having negative PC1 scores, and far sites having more positive PC1 scores (Fig. 2.6). PC2 explained 16% of variance and was positively associated with δ^{13}C-DOC and negatively associated with $SUVA_{254}$ (Fig. 2.6). A passive overlay (using envfit; (Oksanen, 2007)) of modelled water source showed glacial icemelt to be negatively associated with PC1, and snow contributions to be positively associated with PC1; both were associated positively with PC2 (Fig. 2.6). Summer precipitation was negatively associated with PC2 (Fig. 2.6).

2.3.2 Microbial community characterization and its controls over space and time

Generally, microbial communities shared similar dominant classes across sites and seasons with the top ten most abundant phyla across all samples being: Acidobacteriota, Actinobacteriota, Bacteroidota, Bdellovibrionota, Chloroflexi, Cyanobacteria, Firmicutes, Plantomycetota, Proteobacteria, and Verrucomicrobiota (Fig. A.5). Collectively, these ten phyla described between 80-88% of our resolved microbial community composition (Fig. A.5). However, despite

sharing the dominant classes present, microbial communities were less diverse at near sites than at far sites during all seasons, and headwater sites were also less diverse than far sites during the melt season (Fig. A.6.). A comparison of microbial diversity between samples (beta diversity) showed that microbial community composition shifted significantly with movement from headwater and near to far sites data ($R^2 = 0.09$, $p < 0.001$) (Fig. 2.7, Table. A.13). Communities were also distinct across rivers ($R^2 = 0.08$, $p < 0.001$) and different sampling years ($R^2 = 0.06$, $p < 0.001$) with each river and year being significantly different from one other ($p<0.01$) (Fig. A.7, Table. A.13). Nonetheless, a core microbial community was consistently identified across all our samples, regardless of distance range or season sampled. While this core community only represented 3.39% of all identified ASVs, it made up a large fraction of relative abundance at each site (between 25-80%; Fig. 2.8). To explore taxonomic variation at a finer scale we examined the top 10 most abundant shared ASVs, which were identified as belonging to the following families: *Comamonadaceae, Cyanobiaceae, Gallionellaceae, Ilumatobacteraceae, Sporichthyaceae, Alcaligenaceae, Methylophilaceae* and *Flavobacteriaceae*.

To assess whether environmental factors could explain microbial community variance a redundancy analysis was performed. To avoid an over-parameterized model, we omitted highly correlated environmental variables from initial consideration in the redundancy analysis, inputting the following parameters: % protein-like DOM, water temperature, DOC concentration, POC concentration, δ^{13}C-DOC, δ^{18}O-H_2O, d, $S_{275\text{-}295}$, $SUVA_{254}$, TP, TN, and specific conductance; after considering: temperature, pH, specific conductance, turbidity, DOC, DOM composition (% humic-like, FI, BIX, HIX, peak A, peak B, peak C, peak M, peak T, $S_{275\text{-}295}$, $SUVA_{254}$), nutrients (TP, TDN, dSi), major ions (Cl, SO_4, Ca, K, Mg, Na), and metals (Al, Ba, Cr, Mn, Mo, Ni, Sr). The redundancy analysis described a 14% (adjusted) shift in microbial communities, with % protein-like DOM, TN, water temperature, specific conductance, POC and d being significant predictor variables ($p < 0.05$) (Fig. 2.10). RDA axis 1 (RDA1) captured an adjusted 4.6% of sample variation and described a gradient of glacial water inputs, with d and protein-like DOM positively correlated, and specific conductance negatively correlated with this axis (Fig. 2.9). RDA axis 2 (RDA2) described a further adjusted 2.8% of sample variation with TN and water temperature loading negatively on this axis and POC loading positively (Fig. 2.9). Headwater samples had relatively higher scores on both RDA 1 and 2, whereas samples from far sites tended to plot negatively on both axes. Thus, headwater communities were associated with

relatively higher proportions of protein-like DOM and glacial meltwater inputs, and lower specific conductance, water temperature and TN compared to the far sites (Fig. 2.9).

2.3.3 Indicator Species Analysis

An ISA was conducted to identify potential indicator ASVs at headwater, near and far distance sites. Correlations of indicator ASVs with glacial ice contribution revealed that increasing glacial ice contributions drove separation between headwater and far site indicators (Fig. 2.10). Three strong (indicator value (IV) > 0.8) indicator species were resolved for headwater sites and two strong indicator species for far sites ($p < 0.05$). There were no strong indicator species for near sites at this IV threshold. Indicator species for the headwater sites were identified as a species of the genus *Cryobacterium* (IV = 0.89), a species of the family *Beggiatoaceae* (IV = 0.82), and a species of the family *Microbacteriaceae* (IV = 0.87). Far indicators were a species in the family *Sporichthyaceae* (IV = 0.83), and a species in the genus *Cyanobium_PCC-6307* (IV = 0.83).

The strong indicator species (IV > 0.8) that were identified at the headwater sites were correlated ($p < 0.05$) with various stream characteristics (Fig. 2.11). All headwater indicator species were negatively correlated with water temperature, while *Cryobacterium sp*. and *Microbacteriaceae* sp. were additionally negatively correlated with Cl, K, Mg, Na, TN, dSi, and humic-like DOM, and positively correlated with protein-like DOM (Fig. 2.11). *Cryobacterium sp.* was positively correlated with glacial icemelt fraction (Fig. 2.11). Far site indicator species were positively correlated with dSi, SO_4 and Na (Fig. 2.11).

2.4 Discussion

2.4.1 Changing OM quantity with changing water sources

Stream OM originates from two primary sources: 1) *in-situ* primary production of OM from phytoplankton, algae or macrophytes (autochthonous carbon); or 2) OM transported into the stream system from outside sources such as nearby vegetation and soils. In glacially-fed streams, glacially exported OM also forms a portion of the autochthonous carbon pool. In glacial environments themselves, varied carbon sources are present as a result of *in-situ* microbial metabolism on the glacier surface (supraglacial) and at the glacier bed (subglacial) (Hotaling et al., 2017; Stibal et al., 2012), as well as from wind-blown deposition on the snow and ice surface and from comminuted sediments and bedrock material at the bed (Hood et al., 2020; Stubbins et

al., 2012). Thus, the source of water to streams can alter alpine fluvial OM pools as DOM and POM from the source environment can become entrained in water draining into streams (Fasching et al., 2016). At the headwater sites, glacial icemelt contributes a large proportion of the overall stream flow (Fig. A.4). Simultaneously, the distinct lack of input from groundwater (Arendt, 2015), vegetation, and developed soils at these sites combines to make glacially-exported OM a large contribution of allochthonous carbon in the headwater streams. Moving away from the glacier terminus, we observe increased inputs from water derived from precipitation (Fig. A.4) to the fluvial network. We expect that, as is typical for Rocky Mountain streams, water present in downstream rivers is sourced from the surrounding region, with periods of increased transport of water through catchment soils (e.g., spring freshet) (Spencer et al., 2021). During times with lower downstream streamflow (e.g., during the later summer post-melt period) we expect downstream sites to have increasing water additions from deeper soil drainage networks (Paznekas & Hayashi, 2016; Spencer et al., 2021). Thus, reasonably, a fraction of downstream OM will be derived from nearby soils and vegetation, with flow path depth depending on season (i.e., presence or absence of constraining frozen ground layer) and hydrology (i.e., degree of soil saturation).

In this study, we observed low concentrations of DOC across all hydrological periods at the Athabasca glacier headwaters (0.1 to 1 mg L^{-1}) relative to a meta-analysis of 193 North American rivers (average, 4 mg L^{-1}) (Dai et al., 2012) . This finding is expected due to the lack of developed soils at the headwater sites, and is in accordance with previous work in the Alps, Tibetan Plateau, Canadian Rockies and the Greenland Ice sheet that has identified glacial meltwater as a dilute source of OC (Zhang et al., 2018). Increasing DOC concentrations with increasing distance downstream supports the presence of additional carbon inputs from surrounding vegetation and more developed soils. However, overall, the DOC concentration across study sites examined here was still low, which is typical for high elevation locations that experience fast water transit through soils with steep slopes (Laudon et al., 2012). Of note, DOC comprised a larger fraction of the TOC pool further downstream, relative to the headwater site, where POC was frequently the larger contributor to TOC (Fig. 2.2). In inland waters, DOC typically represents a larger portion of TOC relative to POC, as a result of microbial decomposition of soil detrital biomass releasing high amounts of soluble compounds (Lau, 2021). However, in glacially-influenced headwaters POC may be relatively more important due

to increased erosional processes in high slope environments typical of glacial margins, export of glacially-derived sediments (Hood et al., 2020) and higher rates of particle re-suspension in these high-gradient, turbulent, reaches (Marcus et al., 1992).

2.4.2 Shifting sources of carbon to glacially-fed fluvial networks with season and distance

At the Athabasca glacier headwaters, regardless of season, protein-like fluorescence was high, which is consistent with microbial production or microbial reworking of DOM, either on the glacier surface or the bed, being a dominant contributor to the DOM pool (Table. 2.1). High proportions of protein-like fluorescence in glacial meltwaters have been observed in many other glacierized regions (e.g., Tibetan Plateau (Zhou et al., 2019), the Canadian Arctic, Norway, Antarctica (Dubnick et al., 2010), Alaska (Hood et al., 2009; Stubbins et al., 2012b),Greenland (Pain et al., 2020), European alps (Singer et al., 2012)), indicating that glaciers characteristically export OM primarily produced from microbial sources. Moving downstream, the proportion of protein-like DOM decreased and was replaced with increased humic-like fluorescence. This shift was likely tied to the increase in developed vegetation and soil in the drainage catchment as seen in other glacially-fed fluvial networks (Zhou et al., 2019). The observed proportional increase in protein-like fluorescence at the near, mid, and far sites as the melt season progressed may reflect increasing *in-situ* production by microbial photoautotrophs, as evidenced by the presence of cyanobacteria DNA in the microbial amplicon libraires from these sites (Fig. A.5), or microbial re-working of humic-like DOM, either within the stream or in catchment soils (Fig. 2.4, Table. 2.1).

2.4.2.1 Potential allochthonous and autochthonous carbon sources to glacially-fed streams

The variable OM sources with movement from glacial headwaters to downstream reaches is also reflected in shifting isotopic signatures along our transects. Since many DOM sources can have overlapping δ^{13}C-OC ranges (Table. 2.1), Δ^{14}C-OC, which yields insight into carbon age, can be utilized in conjunction with δ^{13}C-OC in order to better identify OM source (Raymond & Bauer, 2001). OM processing by heterotrophic microbes does not substantially fractionate δ^{13}C-OC (e.g., Kritzberg et al., 2004) and thus, signatures of microbially-processed DOM are assumed to be the same as their source. Additionally, it is important to note that stream water δ^{13}C and Δ^{14}C are bulk measurements representing a mixture of many OM sources, which can cloud

interpretation of specific sources. Table 2.1 summarizes potential sources to our riverine OM pool, and their likely δ^{13}C-OC, Δ^{14}C-OC, and fluorescent signatures.

Table 2.1: Potential OC sources to glacially-influenced streams, and their associated expected fluorescence signature and δ^{13}C-OC and Δ^{14}C-OC ranges.

Source	**δ^{13}C-OC**	**Δ^{14}C-OC**	**Expected DOM fluorescence**
Vegetation	-26 to -28‰ (Peterson and Fry, 1987)	Downstream (contemporary) vegetation will be modern whereas subglacial over-ridden vegetation likely represents an aged OC source (Bhatia et al., 2013)	Humic-like (Gabor et al., 2014)
Soils and associated pore water	-26 to -28‰ (Peterson and Fry, 1987)	Modern at the surface with increasing age with depth (Shi et al., 2020)	Humic-like with decreasing humification and increasing protein-like fluorescence with depth and increased soil residence time (Gabor et al., 2014) (McDonough et al., 2022)
Phytoplankton	-22 to -30‰ (Chanton & Lewis, 1999)	Ranging from modern to slightly aged depending on CO_2 source	Protein-like (Fellman et al., 2010)
Benthic algae	Greater than -7 to -15‰ due to decreased isotopic fractionation, following carbon limitation associated with benthic boundary layers (Hecky & Hesslein, 1995)	Ranging from modern to slightly aged depending on CO_2 source	Protein-like (Fellman et al., 2010)
Fossil fuel deposits	-27‰ (Peterson & Fry, 1987)	Ancient (radiocarbon dead)	Variable (Mladenov et al., 2010)
Wildfire derived soot	-26 to -28‰ (Peterson & Fry, 1987)	Modern (Masiello & Druffel, 2003)	Variable (Mladenov et al., 2010)
Chemosynthesis	very depleted -30 to -80‰, via sulfur oxidizing and methanogenic microbes (Blaser & Conrad, 2016; Rau & Hedges, 1979; Ruby et al., 1987)	Ranging from modern to slightly aged depending on the CO_2 source. Notably, subglacial CO_2 can represent an aged C source	Protein-like (Fellman et al., 2010)

2.4.2.2 Seasonally and spatially variable DOM sources to glacially-fed streams and rivers

Water at the Athabasca glacier terminus during the pre-melt period is predominately sourced from the distributed subglacial drainage network (Arendt, 2015), with the DOC pool being aged (Δ^{14}C-DOC = -175‰) and δ^{13}C-DOC depleted (-25.5‰, Fig. 2.4). One potential source of the aged organic material could be over-ridden vegetation and soils entrained in subglacial meltwater, which has been previously proposed to contribute to subglacial runoff in other glacierized regions (e.g., Greenland (Bhatia et al., 2013; Dubnick et al., 2010), the Canadian Arctic, Antarctica (Dubnick et al., 2010)). The protein-like DOM signature could indicate microbial reworking of this aged over-ridden vegetation. The aged (Δ^{14}C-DOC = -200‰), humic-like (δ^{13}C-DOC = -26‰, low % protein-like) signature at the mid-distance site during pre-melt (Fig. 2.4) could indicate contributions from soil water (Table. 2.1). Inputs of modern DOC at the near and mid sites during the pre-melt season may represent increased subsurface flow originating from snowpack melt draining landscapes with well-developed vegetation and soils (Table. 2.1), leading to pulses of concentrated, modern, and terrestrial DOC delivery to streams. The flushing of concentrated DOC from soils was likely the mechanism behind the spike in DOC concentration observed in the pre-melt season at downstream sites in 2019 (Fig. 2.2). This mechanism has been used to explain a similar trend, observed at Bow River from 1998-2000, when the highest DOC concentrations were found to occur during snowpack melt and, as in this study, were followed by a decline in river DOC concentrations (Lafrenière & Sharp, 2004).

Throughout the melt season DOC pools at headwater, near and mid distance sites appeared to switch from being dominated by allochthonous terrestrial inputs (δ^{13}C-DOC = -25 ‰ to -29 ‰) to showing a clear influence of autotrophic sources, likely from chemosynthetic (δ^{13}C-DOC = -29‰ to -35‰) or photoautotrophic microbes (δ^{13}C-DOC = -25‰ to -20‰) (Table. 2.1). If these processes were occurring in a well aerated stream, we would expect a modern, radiocarbon enriched OC pool. However, frequently we observed an old, radiocarbon depleted signature at these sites, which could indicate either DOM sourced from heterotopic consumption of aged metabolism and paired chemolithoautotrophy, or a mixing of aged and modern carbon sources. At the headwater site aged carbon could be accessed from subglacial over-ridden vegetation alongside additions from fossil fuel combustion which have previously been found to be a contributor of DOC in supraglacial meltwater in Alaskan glacial systems (Stubbins et al.,

2012) and glaciers from the Tibetan plateau (Spencer et al., 2014). Aged carbon downstream likely represents the mixing of either 1) aged glacially exported material persisting downstream or 2) additions from deeper soils. Periods when the headwater Δ^{14}C-DOC signature was modern (Fig. 2.4) could indicate increased contributions from supraglacial microbial communities (enriched δ^{13}C-DOC) (Kellerman et al., 2021; Smith et al., 2017; Stibal et al., 2012b) or wildfire derived soot which has previously been found to be deposited on glacier surfaces (Aubry-Wake et al., 2022; Nizam et al., 2020) (Table. 2.1).

During the post-melt period, water at the near and mid distances was aged and displayed variable δ^{13}C-DOC (-22‰ to -29‰, Fig. 2.4) signatures. Aged (Δ^{14}C-DOC = -630‰, 400‰) OM with a δ^{13}C-DOC terrestrial signature (-28‰, -29‰) is consistent with OM contributions from deeper soils during this time when discharge is declining. However, in October 2019, the OC pool was comparatively enriched in δ^{13}C-DOC (-21‰) at the near and mid sites, possibly via additions from benthic primary production (Table 2.1).

2.4.2.3 Stream POC sourced from plant carbon with potential additions from glacier microbes

Compared to the DOC pool, the POC pool at the headwater, near and mid distance sites displayed less variation in δ^{13}C-OC and Δ^{14}C-OC overall, potentially indicating less variation in POC sources to streams. Consistently, across distance ranges and seasons, the POC pool was aged (Δ^{14}C-POC = -550‰ to -108‰) which could indicate sourcing from glacial export of over-ridden vegetation (Bhatia et al., 2013), or fossil fuel products (Stubbins et al., 2012) and the heterotopic consumption of fossil fuels by cryoconite microbes (Margesin et al., 2002). Further downstream, radiocarbon depleted POC could be sourced from the addition of water from aged soil margins (Table. 2.1), or glacially exported aged POM that has persisted through the stream network (Hood et al., 2020). However, δ^{13}C-POC indicated POM mostly of terrestrial plant origin (δ^{13}C‰ = -26 to -28‰, Table. 2.1), with occasional slight depletion (δ^{13}C‰ = -29 to -30‰, Table. 2.1) indicating some additional contribution from subglacial chemosynthetic biofilms (Table. 2.1). If some of the aged POM is sourced from subglacial microbes, this fraction of POM could be more accessible to downstream foodwebs than aged terrestrial POM.

2.4.3 Implications of inferred composition for OM lability

The transition from recently produced, low molecular weight, protein-like DOM to high molecular weight, humic-like DOM with movement from headwater to downstream systems has likely implications for DOM lability (Fig. 2.6). Protein-like DOM is associated with free amino acids and proteinaceous compounds which are generally considered to be more available for heterotrophic microbial consumption, and thus, labile (Coble, 1996). Greater protein-like fluorescence at the headwater and near sites was also associated with increasing inputs from recently produced OM (BIX), and decreasing high molecular weight compounds ($S_{275\text{-}295}$) (Fig. 2.6), two indices also associated with increasing OM lability (Moran & Zepp, 1997; Patriarca et al., 2021). In previous studies of glacial DOM, paired high-resolution mass spectrometry and UV-Vis spectrometry analyses have shown that protein-like fluorescence is associated with unsaturated aliphatic compounds, identified as being peptide-like and lipid-like (Kellerman et al., 2020, 2021; Stubbins et al., 2012b; Zhou et al., 2019). These aliphatic compounds have been found to be a common contributor to glacier DOM pools in many regions, including the Alps (Singer et al., 2012), Greenland (Bhatia et al., 2013; Kellerman et al., 2021), Alaska (Stubbins et al., 2012b), and the Tibetan plateau (Zhou et al., 2019). In contrast, humic-like DOM is associated with complex material (e.g., increased lignin (Mann et al., 2016; Zhou et al., 2019) and thus is generally considered to be a more recalcitrant fraction of DOM, although in some cases can be labile if humic compounds lack protective matrices (Singer et al., 2012)

The lability of OM pools has important implications for stream ecosystems because microbial consumption of DOM can be assimilated to higher trophic levels (e.g., Fellman et al., 2015) and labile DOM has been linked to increased microbial productivity (Pontiller et al., 2020). This relationship between labile DOM, and increased stream productivity due to microbial heterotrophy has been previously observed in glacially-fed streams in the Alps (Singer et al., 2012), and lends credence to the hypothesis that protein-like DOM exported from Rocky Mountain glaciers may be important in stimulating heterotopic stream communities in regional headwaters. Additionally, labile OM released at the headwater site could initiate priming, resulting in increased microbial consumption of recalcitrant soil organic material following additions of labile glacial DOM (Bingeman et al., 1953; Guenet et al., 2010). Priming effects have been demonstrated to occur in river incubation experiments (Hotchkiss et al., 2014), although it is uncertain to what extent priming occurs in riverine environments (Bengtsson et al.,

2018) and such priming effects have not yet been observed in glacially-fed streams. Finally, the amount of carbon available for heterotrophic consumption is also an important consideration on the ultimate effect of DOM lability on microbial productivity. At our downstream sites we had smaller proportions of protein-like DOM but higher DOC concentrations overall, yielding ~0.28 mg L^{-1} of protein-like DOM downstream compared to ~0.21 mg L^{-1} of protein-like DOM at the headwaters (calculated using the mean DOC and % protein-like for that distance bin, and assuming all DOC is fDOM). Therefore, it is unlikely that heterotopic communities at headwater sites would have enhanced productivity over downstream site communities.

2.4.4 Identified dominant microbial phyla common in freshwater and glacial environments

Microbial communities and OM pools are inherently linked since microbes both contribute to the creation of OM and consume it (Kujawinski, 2011). To further explore this relationship along our river transects, we investigated how microbial community composition shifts with increasing distance from glaciers and changing OM source and character. Across all sites and seasons, 10 phyla were found to account for 80 - 88% of community composition (Fig. A.5). While some of these phyla (Actinobacteria, Acidobacteriota, Cyanobacteria, Bacteroidota, and Proteobacteria) are ubiquitous in freshwater (Tamames et al., 2010), many (Proteobacteria, Bacteroidota, Acidobacteriota, Actinobacteriota, Chloroflexi, Cyanobacteria and Firmicutes, Plantomycetota) are also commonly identified as being dominant in glacial ecosystems and in glacially-fed streams (Boetius et al., 2015; Bourquin et al., 2022; Hotaling et al., 2019). These glacially-associated phyla are known to harbor taxa that are adapted to the environmental conditions typical of glacial environments, such as oligotrophy and cold temperatures (Bourquin et al., 2022).

2.4.5 Microbial community structured by environment and dispersal

We observed that within site (alpha) diversity increased with increasing distance from the glacier, a result consistent with a previous study of stream microbial communities in glacially-fed streams in the Alps (Wilhelm et al., 2013). In this work, the lower alpha diversity near glaciers was attributed to a decrease in the diversity of microbial source pools at higher elevations (e.g., a lack of groundwater contributions at high elevations) and/or harsher upstream environmental conditions (Wilhelm et al., 2013). Microbial community composition also shifted

with increased distance from glacier (beta diversity; Fig. 2.7), as has also been observed in work along stream transects from glacier headwaters to downstream in the Alps (Wilhelm et al., 2013). However, the spatial variation observed in this study only explained a small proportion of community composition, indicating that there was a high degree of similarity between microbial communities across distance bins (perMANOVA r2 = 0.09, $p < 0.001$, Table. A.13).

Across all distance ranges (headwater, near, far) examined in this study, a "core" group of microbial ASVs was always present. This core ASV group (1409 unique ASVs) accounted for only ~3% of the total identified ASVs, but represented a large proportion of average community composition across distance ranges (Fig. 2.8). Across all sites, the most abundant (top 10) microbial species from these core taxa display diverse metabolisms, with some heterotopic taxa having species that are considered to be generalists (e.g., *Flavobacterium* (Zheng et al., 2019)*, Sporichthyaceae*), specialists for methanol consumption (*Methylophilaceae* (Beck et al., 2014)), specialists for consumption of terrestrial carbon (*Alcaligenaceae sp.*) and autotrophic taxa, including both photoautotrophs (e.g., cyanobacteria) and chemoautotrophs (e.g., iron oxidizing Gallionellaceae (Hallbeck & Pedersen, 2014)). Though the "core" ASVs were ubiquitous, their relative abundance declined downstream, shifting from a median of 70% of the total community relative abundance at headwater locations to a median of 55% at downstream sites (Fig. 2.8). This pattern persisted within the top 10 taxa of the core, with the average relative abundance of these 10 ASVs being 17.79% at the headwater, 25.77% at near distance and 6.85% at far distance sites (Fig 2.8). Taken together, increases in alpha diversity and declining relative importance of the core community indicates more diverse communities as we move downstream, potentially caused by increased microbial sources from the surrounding terrestrial environment (Fig. A.6).

Redundancy analysis identified water temperature, POC, total nitrogen, d, specific conductance, and protein-like DOM as significant drivers of microbial community composition across sites (Fig. 2.9). Nitrogen and ions associated with specific conductance (e.g Ca, Mg) are essential to microbial growth (Merchant & Helmann, 2012), DOM character can select for different specialized heterotrophic microbes (Judd et al., 2006), and water temperature broadly controls microbial activity (D'Amico et al., 2006). Glacial meltwater contributions can impact community structure both from altering stream abiotic factors (e.g., water temperature, conductivity, nutrients (Milner et al., 2017)) and from being a source of unique glacially sourced microbes (Wilhelm et al., 2013). Finally, POC can shape microbial community composition

because extracellular enzymes are required for bacteria to consume POC (Kellogg & Deming, 2014). Although significant drivers of microbial community composition did exist, together these factors explained only a small amount (14%) of the observed variation in community structure (Fig. 2.9), which is line with a recent synthesis effort that concluded environmental drivers are not always good predictors for microbial community composition in streams (Zeglin, 2015). Since rivers are highly connected environments that can facilitate high rates of dispersal (Tonkin et al., 2018), mass effects can be strong drivers of microbial community composition in fluvial networks causing community homogenization and decreased species sorting (Crump et al., 2007; Evans et al., 2017; Leibold et al., 2004; Pandit et al., 2009). Thus, mass effects may be a strong driver of microbial community composition in our study rivers explaining the modest variation in microbial community structure with shifting environmental conditions, and supported by the identified "core community" that shows clear persistence along our 100 km transects.

2.4.6 Heterotopic headwater indicators positively correlated with protein-like DOM

At sites far downstream from glaciers a large proportion of the upstream community is retained (as described above), however some of the species unique to the headwater site are lost (Fig. 2.8). An indicator species analysis of microbial communities associated with our different distance ranges (headwater, near, far) identified three strong (IV > 0.80) microbial indicators for the headwater site. Headwater indicators *Microbacteriaceae sp.* and *Microbacteriaceae cryobacterium* are commonly identified within glacial cryoconite holes and have been found to possess adaptations for cold temperatures and nutrient poor conditions (Liu et al., 2020). Accordingly, these indicator taxa were found to be negatively correlated with nutrients and ions (dSi, Ca, K, Mg, Na) and warmer temperatures in this study. The other headwater indicator was identified as a sulfur oxidizing chemolithotroph (*Beggiatoaceae sp*), likely sourced from the subglacial environment where chemosynthesis is common (Anesio et al., 2017). The identification of these indicators at headwater sites suggests that glacially-derived microbes (both from the supraglacial and subglacial environment) could be seeding the microbial community at the glacial headwaters (see also Wilhelm et al. 2013). In addition to the relationships between indicator taxa and nutrients, ions, and temperature, we found protein-like DOM to be significantly and positively correlated with heterotopic headwater indicators (Fig. 2.11), non-

significantly and negatively correlated with downstream indicators (Fig. 2.11) and to result in an overall community shift associated with distance range (Fig. 2.9). Thus, some part of the shift in microbial community structure with distance downstream could be due to the loss of glacially-derived specialist species adapted to glacial, protein-like DOM sources.

2.4.7 Implications for or OM pools and microbial communities with glacial retreat

With increased glacier retreat in the Canadian Rockies, rivers with glacial headwaters will shift from a glacier icemelt regime towards one dominated by snow and rainwater inputs (Arendt, 2015) with accompanying increases in water temperatures, soil development and vegetation cover. The collective result of this change is that headwater stream ecosystems will come to resemble our downstream sites more closely. The loss of glacial meltwater inputs will also alter the quantity, age, and character of stream OM pools (Fig. 2.2). Currently, the OM at the glacial headwater was pre-dominantly protein-like throughout the studied hydrologic seasons (pre-melt, melt, post-melt) (Fig. 2.2). As glacial recession leads to declining meltwater contributions coupled with soil development a higher proportion of humic-like DOM at the headwater site is likely. Warmer stream temperatures might lead to more *in-situ* production, heterotrophic consumption, and mineralization. Additionally, it is predicted that there will be a loss of glacially-derived POM into downstream systems which might be bioavailable to primary consumer organisms, which can typically feed directly on POM (Cotner & Biddanda, 2002). Collectively, these results indicate that upstream OM character and sources will become more similar to downstream OM pools with glacier retreat leading to a reduction of beta diversity for both organisms and environmental condition.

Rocky Mountain alpine stream microbial community structure will also likely be impacted by glacier retreat and this will occur primarily via two mechanisms. First, a loss of glacially exported microbes will alter the seed pool available to downstream communities and this could cause microbial community shifts which may persist far downstream (through mass effect processes, as evidenced by the large core community). Second, changing stream physiochemical characteristics associated with glacier loss (such as increased stream temperature, nutrient availability, and conductivity, and changing organic matter composition), will likely also result in an altered community composition as specially adapted microbial taxa are no longer able to compete. Overall, glacier retreat and eventual deglaciation will lead to a

loss of microbial biodiversity in the Canadian Rockies, similar to predictions for other glacierized Alpine regions (Hotaling et al., 2017). This biodiversity loss at the base of stream food webs could have a negative impact on overall riverine ecological stability and downstream ecosystem services via the loss of unique metabolic functions.

2.5 Conclusions

This study illustrates that fluvial OM quantity and quality changes along stream transects from glacier headwaters to ~100 km downstream in the Rocky Mountains. These changes occur as a result of shifting inputs from different OM sources, with headwater sites adjacent to the glacier containing DOM that is compositionally consistent with predominantly autotrophic inputs (chemosynthesis and photosynthesis) and microbial reworking of terrestrially-sourced OM. Throughout the summer melt season, glacially exported OM consistently had high proportions of protein-like DOM, indicating that glacial headwater OM is likely labile. Comparatively, the downstream DOM pool was predominately humic-like, and exhibited seasonal shifts in apparent OM source with allochthonous inputs common in the pre-melt and post-melt seasons, and autochthonous sources increasing at the height of the melt season, potentially sourced from benthic algae production. This study also identified that a portion of glacially-exported POC may be sourced from microbial activity, which could imply that a fraction glacially-exported POC is accessible to downstream food webs. Overall, findings from this study will enable better predictions about the impacts of glacial retreat on stream ecosystems, and, in particular, the loss of labile OM inputs in headwater regions.

As glaciers disappear, there will likely be a shift in microbial community structure. This can be caused both via the direct loss of glacially-exported microbes into headwater systems and through a changing stream environment caused by glacial retreat (e.g., loss of protein-like DOM, warmer stream temperatures, and increased ion and nutrient delivery) (Fig. 2.9). These community shifts may have as yet unquantified impacts on microbial community dynamics, as rare taxa often disproportionality contribute to community functionality (Wilhelm et al., 2013). Finally, the loss of unique functions associated with declines in microbial biodiversity could have larger ecosystem impacts since many of these functions are yet to be identified (Bourquin et al., 2022).

2.6 Figures

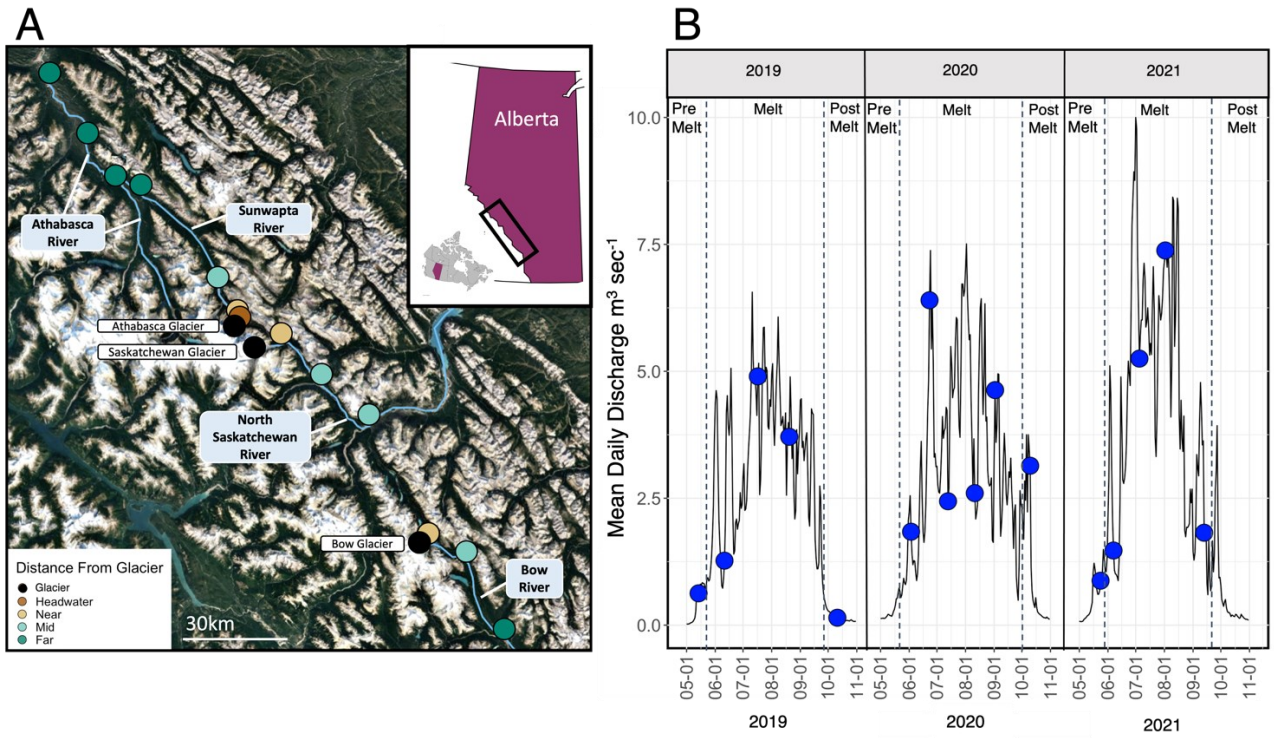

Figure 2.1: (A) Sampling locations of study sites on the Bow North Saskatchewan, Sunwapta, and Athabasca Rivers, in Alberta, Canada (Google Earth © 2022). Locations are coloured by distance range, as outlined in the text. The inset map shows the location of the sampling region (black box) within Alberta. (B) Hydrographs of open-water discharge measured at the gauging station three km downstream of Athabasca glacier (maintained by Environment and Climate Change Canada) from May to November 2019-2021. The location of the hydrologic station corresponds to the Sunwapta "near" site. Sample collection dates are demarcated by blue dots.

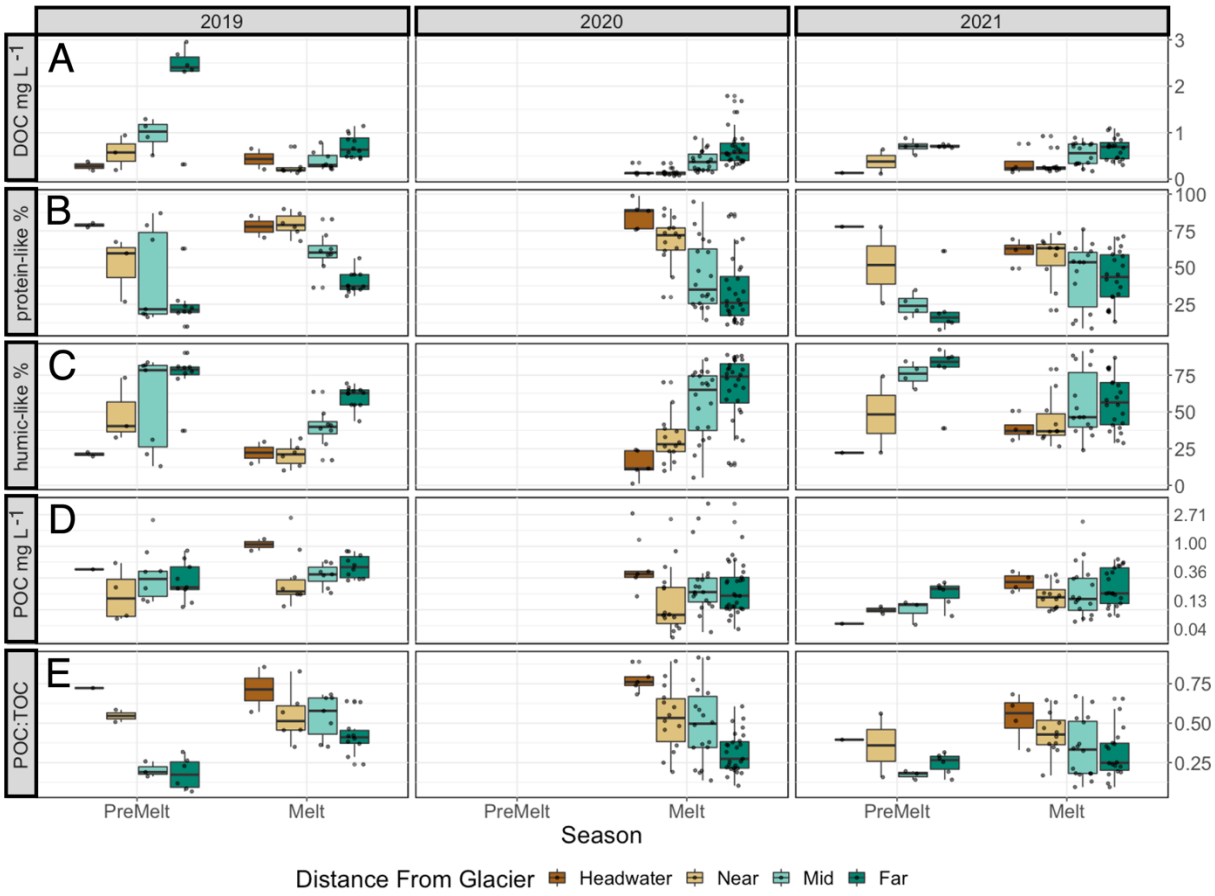

Figure 2.2: Boxplots of: (A) DOC concentration, in mg L^{-1} (B) relative percentage (%) of protein-like DOM (C) relative percentage (%) of humic-like DOM (D); POC concentration in mg L^{-1} (shown on a log scale); and (E) the ratio of POC to TOC (POC + DOC). Data are shown for pre-melt and melt seasons during 2019-2021 across distance ranges. Pre-melt samples in 2020 are missing due to a delay in the field season start because of the Covid-19 pandemic. The boxes represent the inter-quartile range, the black line represents the median value, and individual dots show all collected samples.

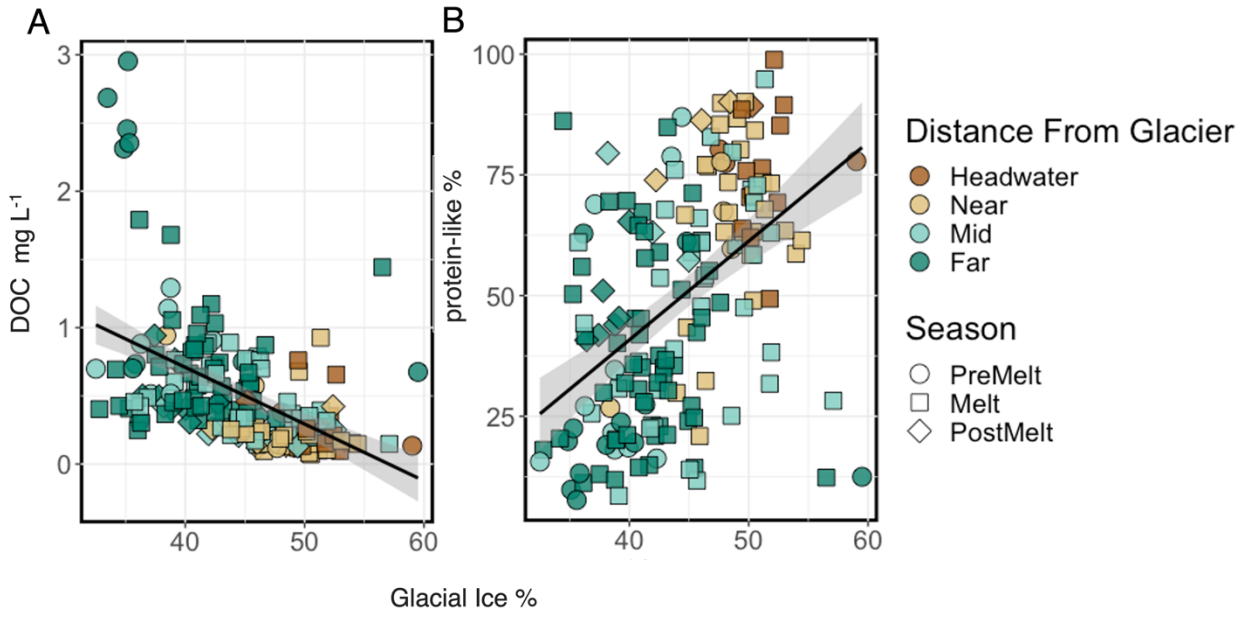

Figure 2.3: The relationship between (A) DOC concentration (mg L^{-1}), and (B) the relative percentage of protein-like DOM (%) and the calculated percentage of glacial ice (%) within streams. Colours represent distance ranges and shapes represent hydrological period. The black line shows a linear fit (DOC = -4.15glacial ice + 2.37, $R^2_{adj} = 0.25$, $p < 0.001$; protein-like% = 2.00glacial ice – 0.4, $R^2_{adj} = 0.22$, $p = <0.01$), with the grey shading demarking the 95% confidence interval.

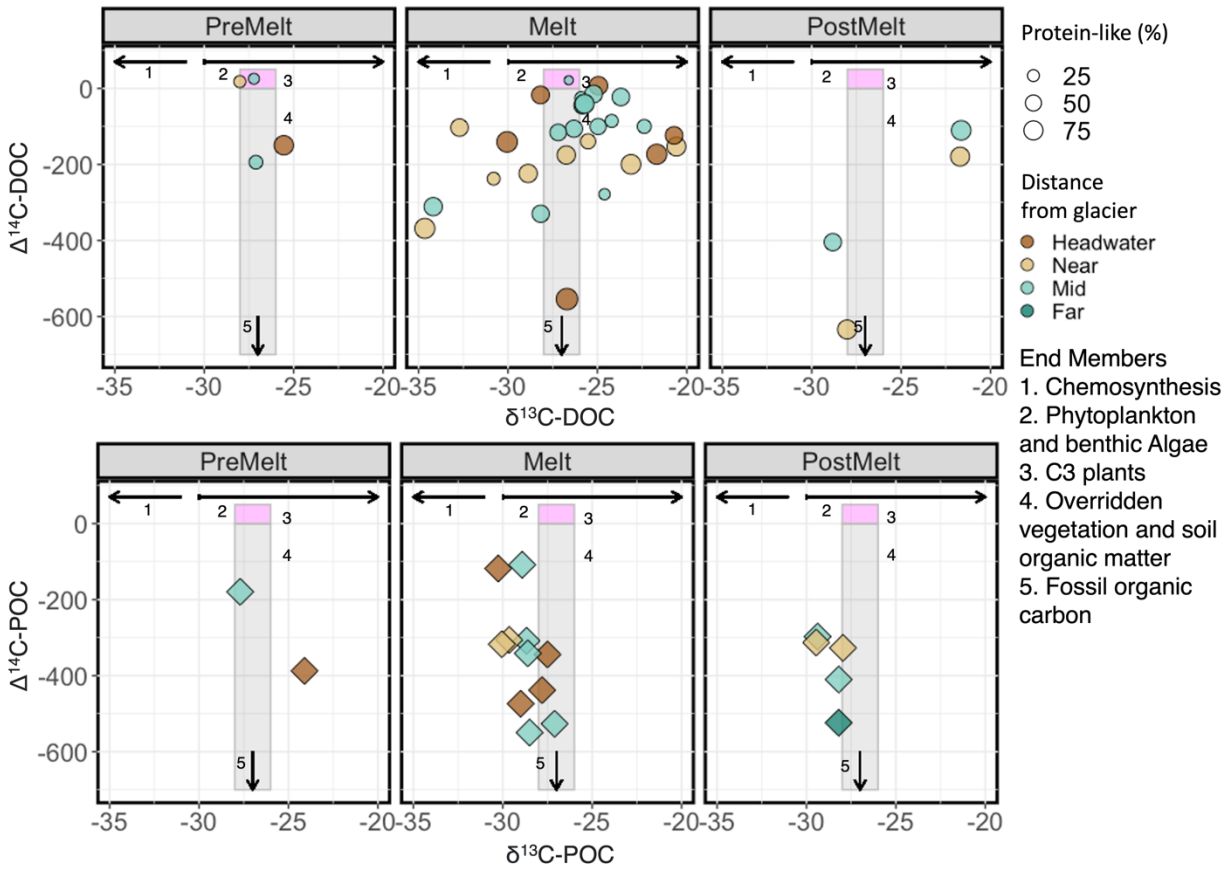

Figure 2.4: $\Delta^{14}C$ versus $\delta^{13}C$ values for (A) dissolved OC with size indicating the percentage protein-like DOM (%) in each sample and (B) particulate OC. Note that symbol size variation is not applicable in panel B. Different colours represent distance ranges. Numbered (1-5) pink and grey boxes and black lines represent literature isotopic ranges for various endmembers (Table. 2.1).

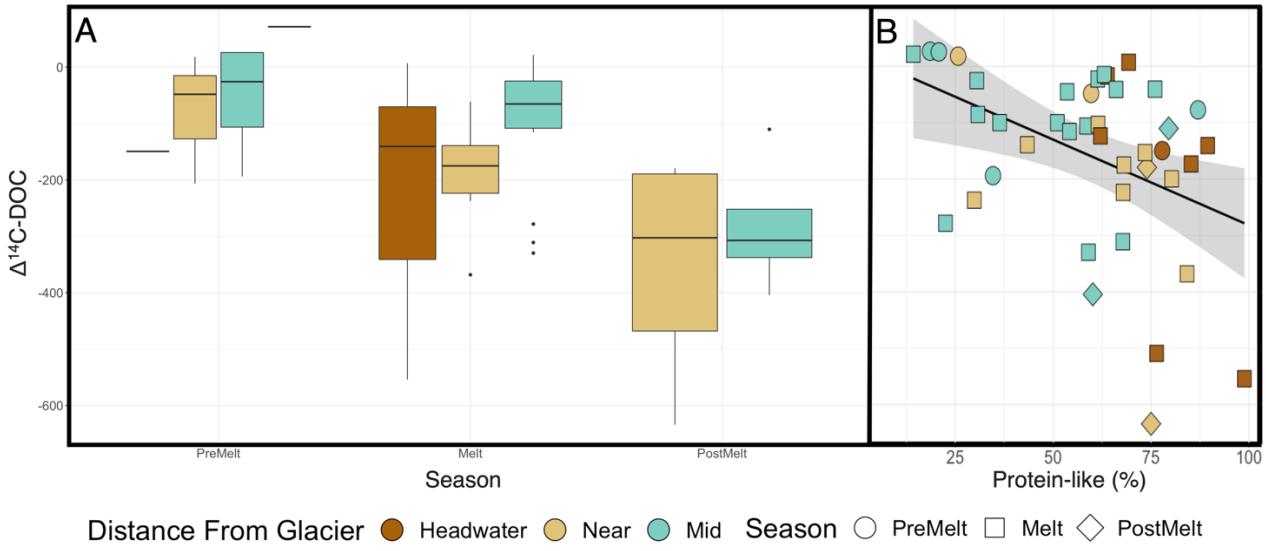

Figure 2.5: (A) Boxplots of stream Δ^{14}C-DOC values for pre-melt, melt and post-melt hydrological periods grouped by distance range. The boxes represent the interquartile range, the black line represents the median value, and the points represent outliers. (B) The correlation between stream Δ^{14}C-DOC and the relative percentage of protein-like DOM (%). Colours represent distance range and shapes represent hydrological periods. The black line shows a linear fit (% protein-like = -303.72 Δ^{14}C-DOC + 21.70, R^2_{adj} = 0.15, p = 0.006), with the grey shading demarking the 95% confidence interval.

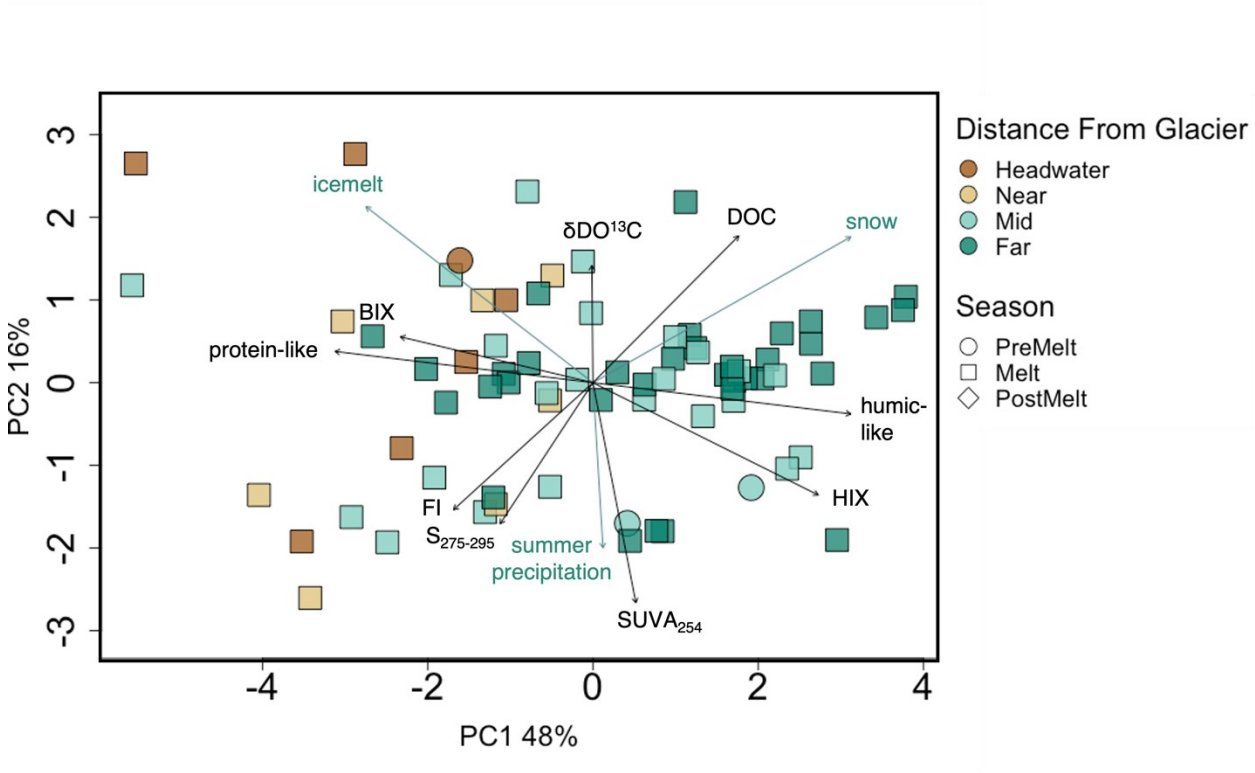

Figure 2.6: Principal component analysis of dissolved OM parameters (DOC concentration, δ^{13}C-DOC, $S_{275\text{-}295}$, $SUVA_{254}$, BIX, FI, HIX, protein-like DOM, and humic-like DOM). Black arrows show ordinated parameters, and the green arrows show water source contributions from the water isotope model that were fitted to the existing PCA. Colours represent distance range, and shapes represent hydrological period.

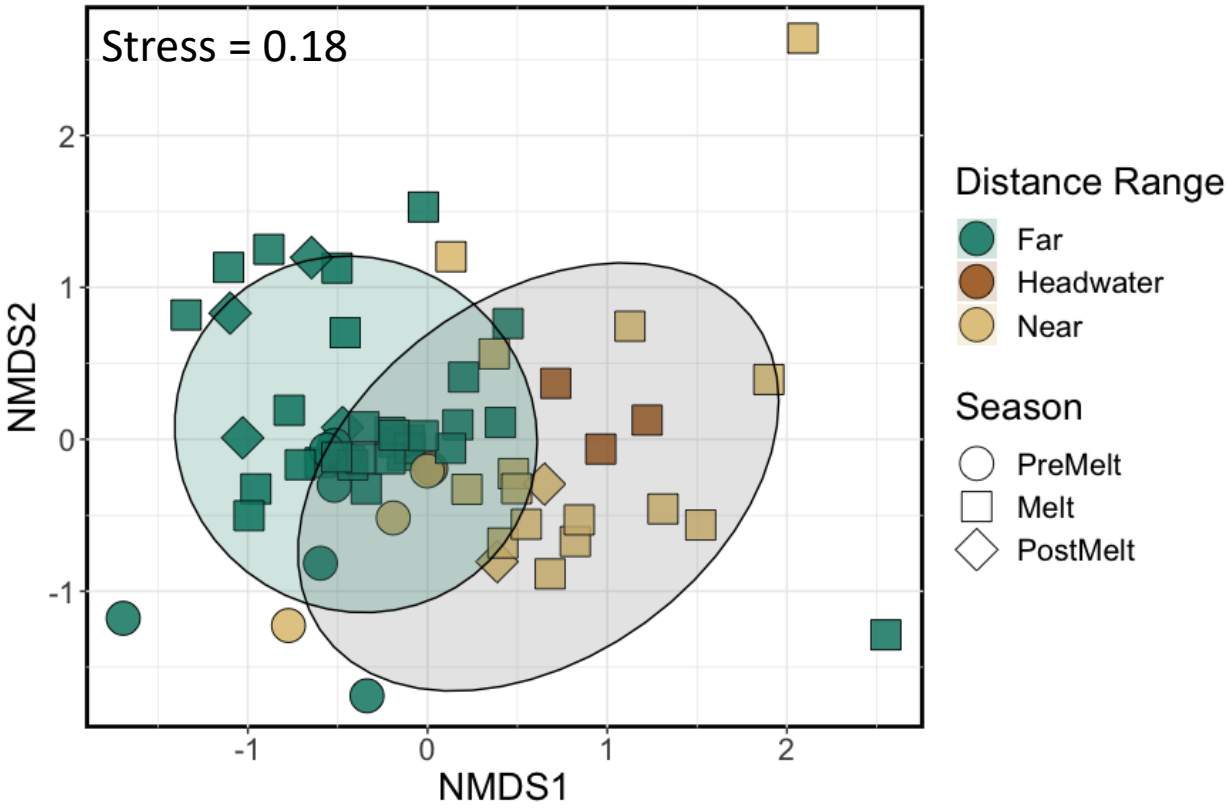

Figure 2.7: (A) NMDS of microbial community composition of stream samples. Shapes represent different hydrological periods while colour indicates distance range. Shaded circles represent the 95% confidence interval for significantly different groupings (pairwise permanova $p < 0.01$ (holms adjusted) see Table. A.13).

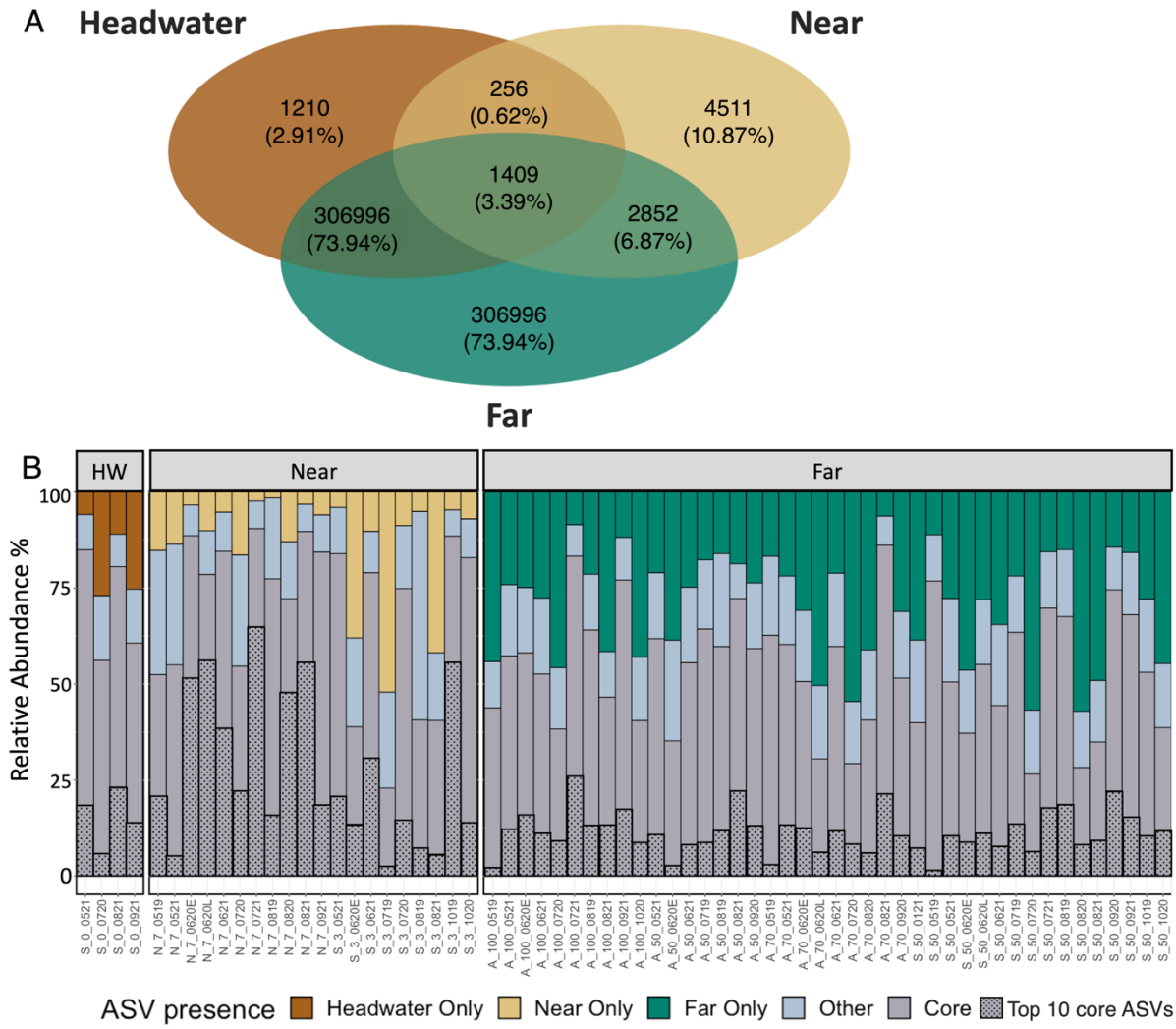

Figure 2.8: (A) Venn diagram showing the number of identified ASVs at the headwater (n = 4 total samples), near (n = 20) and far sites (n = 42). (B) Bar plot showing the relative abundance of ASVs that are unique to each distance range, those ASVs identified in all three (headwater, near, far) distance bins ("core") or those that are shared between two distance bins ("other") in each sample. Sample abbreviations on the x-axis indicates river (Sunwapta (S), North Saskatchewan (N), Athabasca (A)), distance downstream (in km?), and sample date (as mmyy).

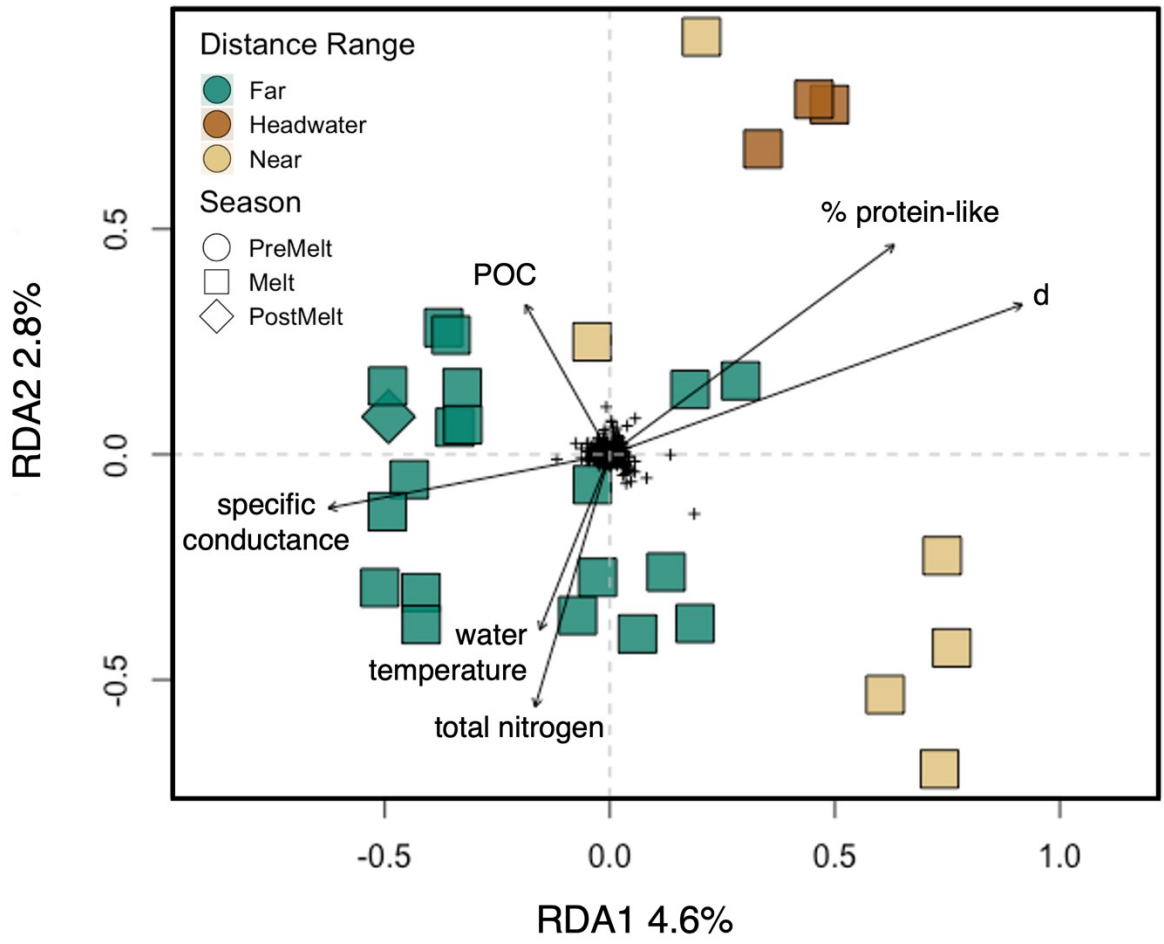

Figure 2.9: Redundancy analysis of microbial community composition at the headwater, near, and far sites constrained by environmental variables, with black arrows showing significant explanatory variables as determined by a backward selection analysis (see methods). Colours represent distance range and shapes represent hydrological period. Black dots in the centre represent individual ASV scores.

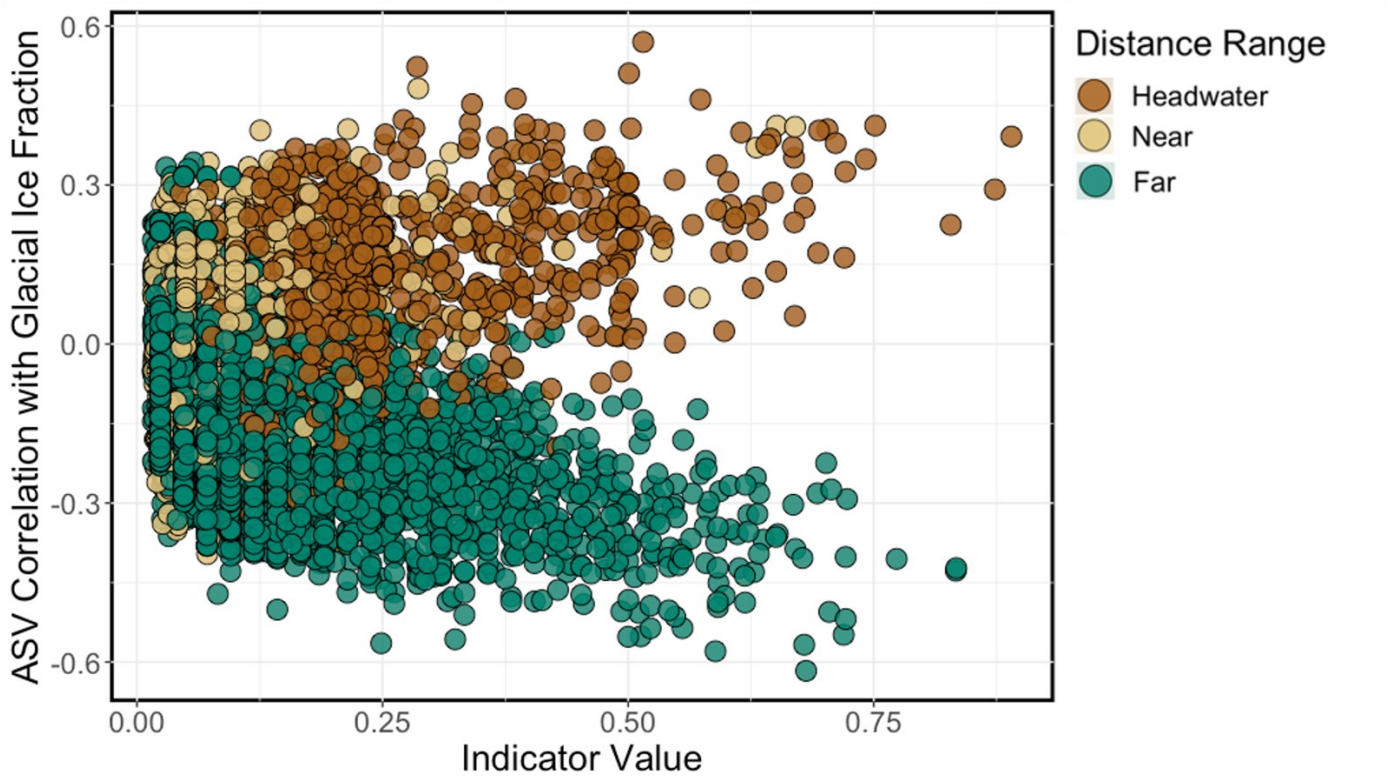

Figure 2.10: A scatterplot of the relationship between the Spearman's rank correlation coefficient for ASV relative abundance and glacial melt fraction, and ASV indicator species value. Brown, beige, and green circles represent the ASVs resolved in the headwater, near and far samples, respectively.

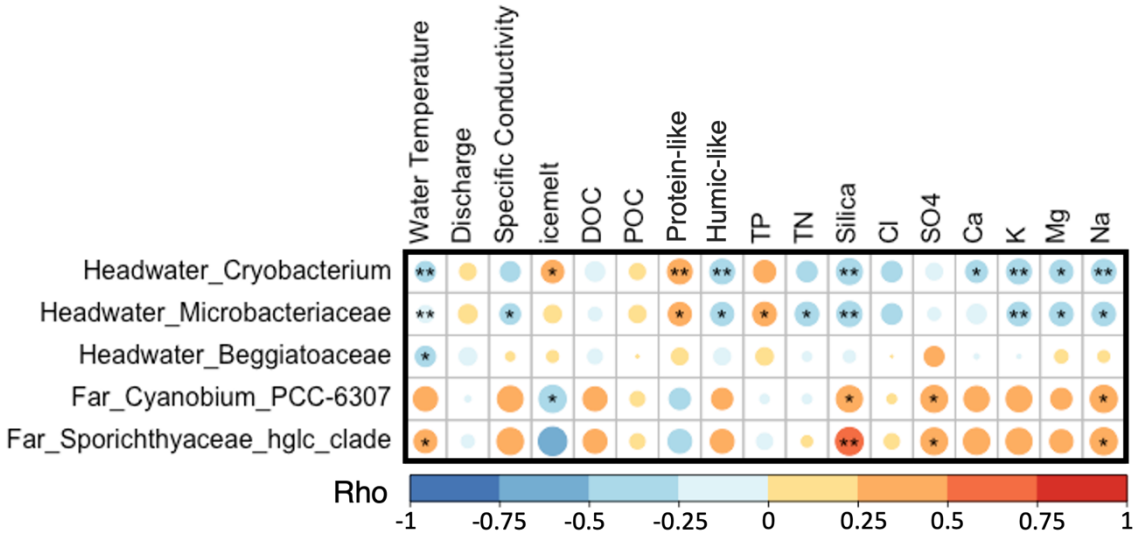

Figure 2.11: Spearman's rank correlations (Rho) between the abundance of strong microbial indicator species (IV > 0.80) and environmental parameters. Stars represent significance level, with $p < 0.05$ (*), and $p < 0.01$ (**) indicated.

Chapter 3: General Conclusion

3.1 Summary of Findings

The objective of this thesis was to investigate the spatial-temporal variations in OM pools and their association with microbial community structure within glacially-sourced streams in the Canadian Rockies. The overarching goal was to generate knowledge to increase understanding of how these alpine streams may be impacted by rapid glacial retreat. My findings suggest that OM at and near glaciers will exhibit changes in quantity, source, and character with deglaciation, and that these changes could potentially cause a loss in microbial diversity with unknown ecosystem impacts.

Across this three-year study, sources, quantity, and character of stream OM was consistently found to change with increased distance from glacier. At and near the glacier headwater I observed low DOC concentrations and high proportions of protein-like fDOM, with isotopic composition consistent with OM sourcing from either primary production from glacier microbes or re-working of aged DOM derived from over-ridden vegetation or fossil fuels. In contrast, at sites further downstream I identified increasing DOC concentrations and an increased proportion of humic-like DOM, with apparent seasonal shifts in contributions from allochthonous to autochthonous OM sources. Changes in water source contributions from glacial ice to precipitation routed through developed soils with increasing distance downstream is the likely driver for shifting OM character. This study also identified that a portion of glacially-exported POM may be sourced from chemosynthetic microbial sources, which could imply that subglacial-exported POM could accessible to downstream food webs. These results indicate that as sites at and near glaciers begin to transition to resemble downstream environments through changing temperature, hydrological, and landscape regimes, it is likely that upstream OM pools will also begin to resemble downstream OM pools more closely, leading to a reduction of beta diversity for both organisms and environmental condition.

Ultimately, only a small amount of microbial community variation was able to be explained by seasonal, spatial, or environmental factors, which is not uncommon in fluvial networks (Zeglin, 2015). This could point to mass effects being a strong determinant of microbial community composition in Rocky Mountain stream environments. This explanation is plausible as rivers represent highly connected networks which can facilitate high levels of

dispersal (Tonkin et al., 2018), leading to a homogenized microbial community across heterogenous environmental gradients. Despite this, my study also resolved strong heterotrophic microbial indicator species for the headwater stream environment that were correlated with protein-like DOM, low nutrients and ions (dSi, TN, K, Mg, Na) and cold temperatures. These headwater indicator species have previously been found to possess cold-adaptations (Liu et al., 2020) and chemolithoautotrophic metabolisms (Teske & Salman, 2014) which could indicate that these taxa may be sourced from the glacier ecosystem. As glaciers disappear and upstream environmental conditions change it is likely that a novel component of the stream microbial community will also be lost.

3.2 Considerations for future research

This study was able to identify a small correlational relationship between microbial community composition and OM characteristics. However, due to the nature of our field sampling design and bulk carbon analytical techniques we are unable to determine which portion of the OM pool is being consumed by microbes, and how microbes are altering the OM characteristics. Future research utilizing experimental approaches could address these outstanding mechanistic questions. Finally, this study used bulk techniques to provide a first assessment of OM composition and microbial community composition across a large spatial and seasonal gradient in the Canadian Rockies. Considerations for future research would be to apply higher resolution approaches to assess DOM composition (e.g., via Fourier-transform ion cyclotron resonance mass spectrometry (FT-ICR-MS)) and better understand active microbial community functioning (e.g, using meta-omic approaches).

Literature Cited

Anderson, S., & Radić, V. (2020). Identification of local water resource vulnerability to rapid deglaciation in Alberta. *Nature Climate Change*, *10*(10), Article 10. https://doi.org/10.1038/s41558-020-0863-4

Anesio, A. M., Lutz, S., Chrismas, N. A. M., & Benning, L. G. (2017). The microbiome of glaciers and ice sheets. *Npj Biofilms and Microbiomes*, *3*(1), Article 1. https://doi.org/10.1038/s41522-017-0019-0

Arendt, C. A. (n.d.). *The Hydrologic Evolution of Glacial Meltwater: Insights and Implications from Alpine and Arctic Glaciers*. 190.

Aubry-Wake, C., Bertoncini, A., & Pomeroy, J. W. (2022). Fire and Ice: The Impact of Wildfire-Affected Albedo and Irradiance on Glacier Melt. *Earth's Future*, *10*(4), e2022EF002685. https://doi.org/10.1029/2022EF002685

Beck, D. A. C., McTaggart, T. L., Setboonsarng, U., Vorobev, A., Kalyuzhnaya, M. G., Ivanova, N., Goodwin, L., Woyke, T., Lidstrom, M. E., & Chistoserdova, L. (2014). The Expanded Diversity of Methylophilaceae from Lake Washington through Cultivation and Genomic Sequencing of Novel Ecotypes. *PLOS ONE*, *9*(7), e102458. https://doi.org/10.1371/journal.pone.0102458

Bengtsson, M. M., Attermeyer, K., & Catalán, N. (2018). Interactive effects on organic matter processing from soils to the ocean: Are priming effects relevant in aquatic ecosystems? *Hydrobiologia*, *822*(1), 1–17. https://doi.org/10.1007/s10750-018-3672-2

Bernhardt, E. S., Savoy, P., Vlah, M. J., Appling, A. P., Koenig, L. E., Hall, R. O., Arroita, M., Blaszczak, J. R., Carter, A. M., Cohen, M., Harvey, J. W., Heffernan, J. B., Helton, A. M., Hosen, J. D., Kirk, L., McDowell, W. H., Stanley, E. H., Yackulic, C. B., & Grimm, N. B. (2022). Light and flow regimes regulate the metabolism of rivers. *Proceedings of the National Academy of Sciences*, *119*(8), e2121976119. https://doi.org/10.1073/pnas.2121976119

Bhatia, M. P., Das, S. B., Longnecker, K., Charette, M. A., & Kujawinski, E. B. (2010). Molecular characterization of dissolved organic matter associated with the Greenland ice sheet. *Geochimica et Cosmochimica Acta*, *74*(13), 3768–3784. https://doi.org/10.1016/j.gca.2010.03.035

Bhatia, M. P., Das, S. B., Xu, L., Charette, M. A., Wadham, J. L., & Kujawinski, E. B. (2013). Organic carbon export from the Greenland ice sheet. *Geochimica et Cosmochimica Acta*, *109*, 329–344. https://doi.org/10.1016/j.gca.2013.02.006

Bingeman, C. W., Varner, J. E., & Martin, W. P. (1953). The Effect of the Addition of Organic Materials on the Decomposition of an Organic Soil. *Soil Science Society of America Journal*, *17*(1), 34–38. https://doi.org/10.2136/sssaj1953.03615995001700010008x

Blaser, M., & Conrad, R. (2016). Stable carbon isotope fractionation as tracer of carbon cycling in anoxic soil ecosystems. *Current Opinion in Biotechnology*, *41*, 122–129. https://doi.org/10.1016/j.copbio.2016.07.001

Boetius, A., Anesio, A. M., Deming, J. W., Mikucki, J. A., & Rapp, J. Z. (2015). Microbial ecology of the cryosphere: Sea ice and glacial habitats. *Nature Reviews Microbiology*, *13*(11), Article 11. https://doi.org/10.1038/nrmicro3522

Boral, S., Sen, I. S., Ghosal, D., Peucker-Ehrenbrink, B., & Hemingway, J. D. (2019). Stable water isotope modeling reveals spatio-temporal variability of glacier meltwater

contributions to Ganges River headwaters. *Journal of Hydrology*, *577*, 123983. https://doi.org/10.1016/j.jhydrol.2019.123983

Bortolini, J., Pineda, A., Rodrigues, L., Jati, S., & Velho, L. (2017). Environmental and spatial processes influencing phytoplankton biomass along a reservoirs-river-floodplain lakes gradient: A metacommunity approach. *Freshwater Biology*, *62*, 1756–1767. https://doi.org/10.1111/fwb.12986

Bourquin, M., Busi, S. B., Fodelianakis, S., Peter, H., Washburne, A., Kohler, T. J., Ezzat, L., Michoud, G., Wilmes, P., & Battin, T. J. (2022). The microbiome of cryospheric ecosystems. *Nature Communications*, *13*(1), Article 1. https://doi.org/10.1038/s41467-022-30816-4

Bowman, S. (1990). *Radiocarbon Dating*. University of California Press.

Cáceres, M. D., & Legendre, P. (2009). Associations between species and groups of sites: Indices and statistical inference. *Ecology*, *90*(12), 3566–3574. https://doi.org/10.1890/08-1823.1

Campbell, D. H., Clow, D. W., Ingersoll, G. P., Mast, M. A., Spahr, N. E., & Turk, J. T. (1995). Processes Controlling the Chemistry of Two Snowmelt-Dominated Streams in the Rocky Mountains. *Water Resources Research*, *31*(11), 2811–2821. https://doi.org/10.1029/95WR02037

Castellazzi, P., Burgess, D., Rivera, A., Huang, J., Longuevergne, L., & Demuth, M. N. (2019). Glacial Melt and Potential Impacts on Water Resources in the Canadian Rocky Mountains. *Water Resources Research*, *55*(12), 10191–10217. https://doi.org/10.1029/2018WR024295

Catalán, N., Casas-Ruiz, J. P., Arce, M. I., Abril, M., Bravo, A. G., del Campo, R., Estévez, E., Freixa, A., Giménez-Grau, P., González-Ferreras, A. M., Gómez-Gener, Ll., Lupon, A., Martínez, A., Palacin-Lizarbe, C., Poblador, S., Rasines-Ladero, R., Reyes, M., Rodríguez-Castillo, T., Rodríguez-Lozano, P., … Pastor, A. (2018). Behind the Scenes: Mechanisms Regulating Climatic Patterns of Dissolved Organic Carbon Uptake in Headwater Streams. *Global Biogeochemical Cycles*, *32*(10), 1528–1541. https://doi.org/10.1029/2018GB005919

Chanton, J. P., & Lewis, F. G. (1999). Plankton and dissolved inorganic carbon isotopic composition in a river-dominated estuary: Apalachicola Bay, Florida. *Estuaries*, *22*(3), 575–583. https://doi.org/10.2307/1353045

Chen, Y., Gu, Y. J., Currie, C. A., Johnston, S. T., Hung, S.-H., Schaeffer, A. J., & Audet, P. (2019). Seismic evidence for a mantle suture and implications for the origin of the Canadian Cordillera. *Nature Communications*, *10*(1), Article 1. https://doi.org/10.1038/s41467-019-09804-8

Clarke, G. K. C., Jarosch, A. H., Anslow, F. S., Radić, V., & Menounos, B. (2015). Projected deglaciation of western Canada in the twenty-first century. *Nature Geoscience*, *8*(5), Article 5. https://doi.org/10.1038/ngeo2407

Coble, P. G. (1996). Characterization of marine and terrestrial DOM in seawater using excitation-emission matrix spectroscopy. *Marine Chemistry*, *51*(4), 325–346. https://doi.org/10.1016/0304-4203(95)00062-3

Cole, J. J., Cole, J. J., Caraco, N. F., & Caraco, N. F. (2001). Carbon in catchments: Connecting terrestrial carbon losses with aquatic metabolism. *Marine and Freshwater Research*, *52*(1), 101. https://doi.org/10.1071/MF00084

Cotner, J. B., & Biddanda, B. A. (2002). Small Players, Large Role: Microbial Influence on Biogeochemical Processes in Pelagic Aquatic Ecosystems. *Ecosystems*, *5*(2), 105–121. https://doi.org/10.1007/s10021-001-0059-3

Coulson, L. E., Weigelhofer, G., Gill, S., Hein, T., Griebler, C., & Schelker, J. (2022). Small rain events during drought alter sediment dissolved organic carbon leaching and respiration in intermittent stream sediments. *Biogeochemistry*, *159*(2), 159–178. https://doi.org/10.1007/s10533-022-00919-7

Crump, B. C., Adams, H. E., Hobbie, J. E., & Kling, G. W. (2007). Biogeography of Bacterioplankton in Lakes and Streams of an Arctic Tundra Catchment. *Ecology*, *88*(6), 1365–1378. https://doi.org/10.1890/06-0387

Crump, B. C., Kling, G. W., Bahr, M., & Hobbie, J. E. (2003). Bacterioplankton Community Shifts in an Arctic Lake Correlate with Seasonal Changes in Organic Matter Source. *Applied and Environmental Microbiology*, *69*(4), 2253–2268. https://doi.org/10.1128/AEM.69.4.2253-2268.2003

Dai, M., Yin, Z., Meng, F., Liu, Q., & Cai, W.-J. (2012). Spatial distribution of riverine DOC inputs to the ocean: An updated global synthesis. *Current Opinion in Environmental Sustainability*, *4*(2), 170–178. https://doi.org/10.1016/j.cosust.2012.03.003

D'Amico, S., Collins, T., Marx, J.-C., Feller, G., & Gerday, C. (2006). Psychrophilic microorganisms: Challenges for life. *EMBO Reports*, *7*(4), 385–389. https://doi.org/10.1038/sj.embor.7400662

D'Andrilli, J., Cooper, W. T., Foreman, C. M., & Marshall, A. G. (2015). An ultrahigh-resolution mass spectrometry index to estimate natural organic matter lability. *Rapid Communications in Mass Spectrometry*, *29*(24), 2385–2401. https://doi.org/10.1002/rcm.7400

Davis, N. M., Proctor, D. M., Holmes, S. P., Relman, D. A., & Callahan, B. J. (2018). *Simple statistical identification and removal of contaminant sequences in marker-gene and metagenomics data* (p. 221499). bioRxiv. https://doi.org/10.1101/221499

Dubnick, A., Barker, J., Sharp, M., Wadham, J., Lis, G., Telling, J., Fitzsimons, S., & Jackson, M. (2010). Characterization of dissolved organic matter (DOM) from glacial environments using total fluorescence spectroscopy and parallel factor analysis. *Annals of Glaciology*, *51*(56), 111–122. https://doi.org/10.3189/172756411795931912

Elser, J. J., Wu, C., González, A. L., Shain, D. H., Smith, H. J., Sommaruga, R., Williamson, C. E., Brahney, J., Hotaling, S., Vanderwall, J., Yu, J., Aizen, V., Aizen, E., Battin, T. J., Camassa, R., Feng, X., Jiang, H., Lu, L., Qu, J. J., … Saros, J. E. (2020). Key rules of life and the fading cryosphere: Impacts in alpine lakes and streams. *Global Change Biology*, *26*(12), 6644–6656. https://doi.org/10.1111/gcb.15362

Environment and Climate Change Canada. (2022). Water Level and Flow [HYDAT database]. Retrieved August 8, 2022, from https://wateroffice.ec.gc.ca/index_e.html

Evans, S., Martiny, J. B. H., & Allison, S. D. (2017). Effects of dispersal and selection on stochastic assembly in microbial communities. *The ISME Journal*, *11*(1), Article 1. https://doi.org/10.1038/ismej.2016.96

Fasching, C., Ulseth, A. J., Schelker, J., Steniczka, G., & Battin, T. J. (2016). Hydrology controls dissolved organic matter export and composition in an Alpine stream and its hyporheic zone. *Limnology and Oceanography*, *61*(2), 558–571. https://doi.org/10.1002/lno.10232

Fellman, J. B., Hood, E., Raymond, P. A., Hudson, J., Bozeman, M., & Arimitsu, M. (2015). Evidence for the assimilation of ancient glacier organic carbon in a proglacial stream

food web. *Limnology and Oceanography*, *60*(4), 1118–1128. https://doi.org/10.1002/lno.10088

Fellman, J. B., Hood, E., & Spencer, R. G. M. (2010). Fluorescence spectroscopy opens new windows into dissolved organic matter dynamics in freshwater ecosystems: A review. *Limnology and Oceanography*, *55*(6), 2452–2462. https://doi.org/10.4319/lo.2010.55.6.2452

Gabor, R. S., Baker, A., McKnight, D. M., & Miller, M. P. (2014). Fluorescence Indices and Their Interpretation. In A. Baker, D. M. Reynolds, J. Lead, P. G. Coble, & R. G. M. Spencer (Eds.), *Aquatic Organic Matter Fluorescence* (pp. 303–338). Cambridge University Press. https://doi.org/10.1017/CBO9781139045452.015

Graeber, D., Gelbrecht, J., Pusch, M. T., Anlanger, C., & von Schiller, D. (2012). Agriculture has changed the amount and composition of dissolved organic matter in Central European headwater streams. *Science of The Total Environment*, *438*, 435–446. https://doi.org/10.1016/j.scitotenv.2012.08.087

Graham, E. B., Knelman, J. E., Schindlbacher, A., Siciliano, S., Breulmann, M., Yannarell, A., Beman, J. M., Abell, G., Philippot, L., Prosser, J., Foulquier, A., Yuste, J. C., Glanville, H. C., Jones, D. L., Angel, R., Salminen, J., Newton, R. J., Bürgmann, H., Ingram, L. J., … Nemergut, D. R. (2016). Microbes as Engines of Ecosystem Function: When Does Community Structure Enhance Predictions of Ecosystem Processes? *Frontiers in Microbiology*, *7*. https://www.frontiersin.org/articles/10.3389/fmicb.2016.00214

Guenet, B., Danger, M., Abbadie, L., & Lacroix, G. (2010). Priming effect: Bridging the gap between terrestrial and aquatic ecology. *Ecology*, *91*(10), 2850–2861. https://doi.org/10.1890/09-1968.1

Hallbeck, L., & Pedersen, K. (2014). The Family Gallionellaceae. In E. Rosenberg, E. F. DeLong, S. Lory, E. Stackebrandt, & F. Thompson (Eds.), *The Prokaryotes: Alphaproteobacteria and Betaproteobacteria* (pp. 853–858). Springer. https://doi.org/10.1007/978-3-642-30197-1_398

Hecky, R. E., & Hesslein, R. H. (1995). Contributions of Benthic Algae to Lake Food Webs as Revealed by Stable Isotope Analysis. *Journal of the North American Benthological Society*, *14*(4), 631–653. https://doi.org/10.2307/1467546

Helms, J. R., Stubbins, A., Ritchie, J. D., Minor, E. C., Kieber, D. J., & Mopper, K. (2008). Absorption spectral slopes and slope ratios as indicators of molecular weight, source, and photobleaching of chromophoric dissolved organic matter. *Limnology and Oceanography*, *53*(3), 955–969. https://doi.org/10.4319/lo.2008.53.3.0955

Hill, M. O. (1973). Diversity and Evenness: A Unifying Notation and Its Consequences. *Ecology*, *54*(2), 427–432. https://doi.org/10.2307/1934352

Hood, E., Battin, T. J., Fellman, J., O'neel, S., & Spencer, R. G. M. (2015). Storage and release of organic carbon from glaciers and ice sheets. *Nature Geoscience*, *8*(2), 91–96. https://doi.org/10.1038/ngeo2331

Hood, E., Fellman, J. B., & Spencer, R. G. M. (2020). Glacier Loss Impacts Riverine Organic Carbon Transport to the Ocean. *Geophysical Research Letters*, *47*(19). https://doi.org/10.1029/2020GL089804

Hood, E., Fellman, J., Spencer, R. G. M., Hernes, P. J., Edwards, R., D'Amore, D., & Scott, D. (2009). Glaciers as a source of ancient and labile organic matter to the marine environment. *Nature*, *462*(7276), Article 7276. https://doi.org/10.1038/nature08580

Hotaling, S., Foley, M. E., Zeglin, L. H., Finn, D. S., Tronstad, L. M., Giersch, J. J., Muhlfeld, C. C., & Weisrock, D. W. (2019). Microbial assemblages reflect environmental heterogeneity in alpine streams. *Global Change Biology*, *25*(8), 2576–2590. https://doi.org/10.1111/gcb.14683

Hotaling, S., Hood, E., & Hamilton, T. L. (2017). Microbial ecology of mountain glacier ecosystems: Biodiversity, ecological connections and implications of a warming climate. *Environmental Microbiology*, *19*(8), 2935–2948. https://doi.org/10.1111/1462-2920.13766

Hotchkiss, E. R., Hall Jr., R. O., Baker, M. A., Rosi-Marshall, E. J., & Tank, J. L. (2014). Modeling priming effects on microbial consumption of dissolved organic carbon in rivers. *Journal of Geophysical Research: Biogeosciences*, *119*(5), 982–995. https://doi.org/10.1002/2013JG002599

Huguet, A., Vacher, L., Relexans, S., Saubusse, S., Froidefond, J.-M., & Parlanti, E. (2008). Properties of Fluorescent Dissolved Organic Matter in the Gironde Estuary. *Organic Geochemistry*, *40*, 706–719. https://doi.org/10.1016/j.orggeochem.2009.03.002

Jones, S. E., Newton, R. J., & McMahon, K. D. (2009). Evidence for structuring of bacterial community composition by organic carbon source in temperate lakes. *Environmental Microbiology*, *11*(9), 2463–2472. https://doi.org/10.1111/j.1462-2920.2009.01977.x

Judd, K. E., Crump, B. C., & Kling, G. W. (2006). Variation in Dissolved Organic Matter Controls Bacterial Production and Community Composition. *Ecology*, *87*(8), 2068–2079. https://doi.org/10.1890/0012-9658(2006)87[2068:VIDOMC]2.0.CO;2

Karstens, L., Asquith, M., Davin, S., Fair, D., Gregory, W. T., Wolfe, A. J., Braun, J., & McWeeney, S. (2019). Controlling for Contaminants in Low-Biomass 16S rRNA Gene Sequencing Experiments. *MSystems*, *4*(4), e00290-19. https://doi.org/10.1128/mSystems.00290-19

Kellerman, A. M., Hawkings, J. R., Wadham, J. L., Kohler, T. J., Stibal, M., Grater, E., Marshall, M., Hatton, J. E., Beaton, A., & Spencer, R. G. M. (2020). Glacier Outflow Dissolved Organic Matter as a Window Into Seasonally Changing Carbon Sources: Leverett Glacier, Greenland. *Journal of Geophysical Research: Biogeosciences*, *125*(4), e2019JG005161. https://doi.org/10.1029/2019JG005161

Kellerman, A. M., Vonk, J., McColaugh, S., Podgorski, D. C., van Winden, E., Hawkings, J. R., Johnston, S. E., Humayun, M., & Spencer, R. G. M. (2021). Molecular Signatures of Glacial Dissolved Organic Matter From Svalbard and Greenland. *Global Biogeochemical Cycles*, *35*(3), e2020GB006709. https://doi.org/10.1029/2020GB006709

Kellogg, C. T. E., & Deming, J. W. (2014). Particle-associated extracellular enzyme activity and bacterial community composition across the Canadian Arctic Ocean. *FEMS Microbiology Ecology*, *89*(2), 360–375. https://doi.org/10.1111/1574-6941.12330

Kritzberg, E. S., Cole, J. J., Pace, M. L., Granéli, W., & Bade, D. L. (2004). Autochthonous versus allochthonous carbon sources of bacteria: Results from whole-lake 13C addition experiments. *Limnology and Oceanography*, *49*(2), 588–596. https://doi.org/10.4319/lo.2004.49.2.0588

Kujawinski, E. B. (2011). The Impact of Microbial Metabolism on Marine Dissolved Organic Matter. *Annual Review of Marine Science*, *3*(1), 567–599. https://doi.org/10.1146/annurev-marine-120308-081003

Lafrenière, M. J., & Sharp, M. J. (2004). The Concentration and Fluorescence of Dissolved Organic Carbon (DOC) in Glacial and Nonglacial Catchments: Interpreting Hydrological

Flow Routing and DOC Sources. *Arctic, Antarctic, and Alpine Research*, *36*(2), 156–165. https://doi.org/10.1657/1523-0430(2004)036[0156:TCAFOD]2.0.CO;2

Lau, M. P. (2021). Linking the Dissolved and Particulate Domain of Organic Carbon in Inland Waters. *Journal of Geophysical Research: Biogeosciences*, *126*(5), e2021JG006266. https://doi.org/10.1029/2021JG006266

Laudon, H., Buttle, J., Carey, S. K., McDonnell, J., McGuire, K., Seibert, J., Shanley, J., Soulsby, C., & Tetzlaff, D. (2012). Cross-regional prediction of long-term trajectory of stream water DOC response to climate change. *Geophysical Research Letters*, *39*(18). https://doi.org/10.1029/2012GL053033

Leibold, M. A., Holyoak, M., Mouquet, N., Amarasekare, P., Chase, J. M., Hoopes, M. F., Holt, R. D., Shurin, J. B., Law, R., Tilman, D., Loreau, M., & Gonzalez, A. (2004). The metacommunity concept: A framework for multi-scale community ecology. *Ecology Letters*, *7*(7), 601–613. https://doi.org/10.1111/j.1461-0248.2004.00608.x

Li, P., & Hur, J. (2017). Utilization of UV-Vis spectroscopy and related data analyses for dissolved organic matter (DOM) studies: A review. *Critical Reviews in Environmental Science and Technology*, *47*(3), 131–154. https://doi.org/10.1080/10643389.2017.1309186

Liu, Y., Shen, L., Zeng, Y., Xing, T., Xu, B., & Wang, N. (2020). Genomic Insights of Cryobacterium Isolated From Ice Core Reveal Genome Dynamics for Adaptation in Glacier. *Frontiers in Microbiology*, *11*. https://www.frontiersin.org/articles/10.3389/fmicb.2020.01530

Luckman, B. H. (2017). Glacier Landscapes in the Canadian Rockies. In O. Slaymaker (Ed.), *Landscapes and Landforms of Western Canada* (pp. 241–255). Springer International Publishing. https://doi.org/10.1007/978-3-319-44595-3_17

Mann, P. J., Spencer, R. G. M., Hernes, P. J., Six, J., Aiken, G. R., Tank, S. E., McClelland, J. W., Butler, K. D., Dyda, R. Y., & Holmes, R. M. (2016). Pan-Arctic Trends in Terrestrial Dissolved Organic Matter from Optical Measurements. *Frontiers in Earth Science*, *4*. https://www.frontiersin.org/articles/10.3389/feart.2016.00025

Marcus, W. A., Roberts, K., Harvey, L., & Tackman, G. (1992). An Evaluation of Methods for Estimating Manning's n in Small Mountain Streams. *Mountain Research and Development*, *12*(3), 227–239. https://doi.org/10.2307/3673667

Margesin, R., Zacke, G., & Schinner, F. (2002). Characterization of Heterotrophic Microorganisms in Alpine Glacier Cryoconite. *Arctic, Antarctic, and Alpine Research*, *34*(1), 88–93. https://doi.org/10.1080/15230430.2002.12003472

Masiello, C. A., & Druffel, E. R. M. (2003). Organic and black carbon 13C and 14C through the Santa Monica Basin sediment oxic-anoxic transition. *Geophysical Research Letters*, *30*(4). https://doi.org/10.1029/2002GL015050

McDonough, L. K., Andersen, M. S., Behnke, M. I., Rutlidge, H., Oudone, P., Meredith, K., O'Carroll, D. M., Santos, I. R., Marjo, C. E., Spencer, R. G. M., McKenna, A. M., & Baker, A. (2022). A new conceptual framework for the transformation of groundwater dissolved organic matter. *Nature Communications*, *13*(1), Article 1. https://doi.org/10.1038/s41467-022-29711-9

McKnight, D. M., Boyer, E. W., Westerhoff, P. K., Doran, P. T., Kulbe, T., & Andersen, D. T. (2001a). Spectrofluorometric characterization of dissolved organic matter for indication of precursor organic material and aromaticity. *Limnology and Oceanography*, *46*(1), 38–48. https://doi.org/10.4319/lo.2001.46.1.0038

McKnight, D. M., Boyer, E. W., Westerhoff, P. K., Doran, P. T., Kulbe, T., & Andersen, D. T. (2001b). Spectrofluorometric characterization of dissolved organic matter for indication of precursor organic material and aromaticity. *Limnology and Oceanography*, *46*(1), 38–48. https://doi.org/10.4319/lo.2001.46.1.0038

Merchant, S. S., & Helmann, J. D. (2012). Elemental Economy: Microbial strategies for optimizing growth in the face of nutrient limitation. *Advances in Microbial Physiology*, *60*, 91–210. https://doi.org/10.1016/B978-0-12-398264-3.00002-4

Milner, A. M., Khamis, K., Battin, T. J., Brittain, J. E., Barrand, N. E., Füreder, L., Cauvy-Fraunié, S., Gíslason, G. M., Jacobsen, D., Hannah, D. M., Hodson, A. J., Hood, E., Lencioni, V., Ólafsson, J. S., Robinson, C. T., Tranter, M., & Brown, L. E. (2017). Glacier shrinkage driving global changes in downstream systems. *Proceedings of the National Academy of Sciences*, *114*(37), 9770–9778. https://doi.org/10.1073/pnas.1619807114

Mladenov, N., Reche, I., Olmo, F. J., Lyamani, H., & Alados-Arboledas, L. (2010). Relationships between spectroscopic properties of high-altitude organic aerosols and Sun photometry from ground-based remote sensing. *Journal of Geophysical Research: Biogeosciences*, *115*(G1). https://doi.org/10.1029/2009JG000991

Moore, R. D., Fleming, S. W., Menounos, B., Wheate, R., Fountain, A., Stahl, K., Holm, K., & Jakob, M. (2009). Glacier change in western North America: Influences on hydrology, geomorphic hazards and water quality. *Hydrological Processes*, *23*(1), 42–61. https://doi.org/10.1002/hyp.7162

Moran, M. A., & Zepp, R. G. (1997). Role of photoreactions in the formation of biologically labile compounds from dissolved organic matter. *Limnology and Oceanography*, *42*(6), 1307–1316. https://doi.org/10.4319/lo.1997.42.6.1307

Murphy, K. R., Stedmon, C. A., Graeber, D., & Bro, R. (2013). Fluorescence spectroscopy and multi-way techniques. PARAFAC. *Analytical Methods*, *5*(23), 6557–6566. https://doi.org/10.1039/C3AY41160E

Murphy, K. R., Stedmon, C. A., Waite, T. D., & Ruiz, G. M. (2008). Distinguishing between terrestrial and autochthonous organic matter sources in marine environments using fluorescence spectroscopy. *Marine Chemistry*, *108*(1), 40–58. https://doi.org/10.1016/j.marchem.2007.10.003

Murphy, K. R., Stedmon, C. A., Wenig, P., & Bro, R. (2014). OpenFluor– an online spectral library of auto-fluorescence by organic compounds in the environment. *Analytical Methods*, *6*(3), 658–661. https://doi.org/10.1039/C3AY41935E

Muscarella, M. E., Boot, C. M., Broeckling, C. D., & Lennon, J. T. (2019). Resource heterogeneity structures aquatic bacterial communities. *The ISME Journal*, *13*(9), Article 9. https://doi.org/10.1038/s41396-019-0427-7

Musilova, M., Tranter, M., Wadham, J., Telling, J., Tedstone, A., & Anesio, A. M. (2017). Microbially driven export of labile organic carbon from the Greenland ice sheet. *Nature Geoscience*, *10*(5), 360–365. https://doi.org/10.1038/ngeo2920

Nelson, D. W., & Sommers, L. E. (1996). Total Carbon, Organic Carbon, and Organic Matter. In *Methods of Soil Analysis* (pp. 961–1010). John Wiley & Sons, Ltd. https://doi.org/10.2136/sssabookser5.3.c34

Nienow, P., Sharp, M., & Willis, I. (1998). Seasonal changes in the morphology of the subglacial drainage system, Haut Glacier d'Arolla, Switzerland. *Earth Surface Processes and*

Landforms, *23*(9), 825–843. https://doi.org/10.1002/(SICI)1096-9837(199809)23:9<825::AID-ESP893>3.0.CO;2-2

Nizam, S., Sen, I. S., Vinoj, V., Galy, V., Selby, D., Azam, M. F., Pandey, S. K., Creaser, R. A., Agarwal, A. K., Singh, A. P., & Bizimis, M. (2020). Biomass-Derived Provenance Dominates Glacial Surface Organic Carbon in the Western Himalaya. *Environmental Science & Technology*, *54*(14), 8612–8621. https://doi.org/10.1021/acs.est.0c02710

Ohno, T. (2002). Fluorescence Inner-Filtering Correction for Determining the Humification Index of Dissolved Organic Matter. *Environmental Science & Technology*, *36*(4), 742–746. https://doi.org/10.1021/es0155276

Oksanen, J. (2007). Vegan: Community ecology package. R package version 1.8-5. *Http://Www. Cran. r-Project. Org*.

Orwin, J. F., Lamoureux, S. F., Warburton, J., & Beylich, A. (2010). A Framework for Characterizing Fluvial Sediment Fluxes from Source to Sink in Cold Environments. *Geografiska Annaler. Series A, Physical Geography*, *92*(2), 155–176.

Pain, A. J., Martin, J. B., Martin, E. E., Rahman, S., & Ackermann, P. (2020). Differences in the Quantity and Quality of Organic Matter Exported From Greenlandic Glacial and Deglaciated Watersheds. *Global Biogeochemical Cycles*, *34*(10), e2020GB006614. https://doi.org/10.1029/2020GB006614

Pandit, S. N., Kolasa, J., & Cottenie, K. (2009). Contrasts between habitat generalists and specialists: An empirical extension to the basic metacommunity framework. *Ecology*, *90*(8), 2253–2262. https://doi.org/10.1890/08-0851.1

Parada, A. E., Needham, D. M., & Fuhrman, J. A. (2016). Every base matters: Assessing small subunit rRNA primers for marine microbiomes with mock communities, time series and global field samples. *Environmental Microbiology*, *18*(5), 1403–1414. https://doi.org/10.1111/1462-2920.13023

Paterson, W. S. B. (1994). 10—Distribution of Temperature in Glaciers and Ice Sheets. In W. S. B. Paterson (Ed.), *The Physics of Glaciers (Third Edition)* (pp. 204–237). Pergamon. https://doi.org/10.1016/B978-0-08-037944-9.50016-9

Patriarca, C., Sedano-Núñez, V. T., Garcia, S. L., Bergquist, J., Bertilsson, S., Sjöberg, P. J. R., Tranvik, L. J., & Hawkes, J. A. (2021). Character and environmental lability of cyanobacteria-derived dissolved organic matter. *Limnology and Oceanography*, *66*(2), 496–509. https://doi.org/10.1002/lno.11619

Paznekas, A., & Hayashi, M. (2016). Groundwater contribution to winter streamflow in the Canadian Rockies. *Canadian Water Resources Journal / Revue Canadienne Des Ressources Hydriques*, *41*(4), 484–499. https://doi.org/10.1080/07011784.2015.1060870

Peterson, B. J., & Fry, B. (1987). Stable Isotopes in Ecosystem Studies. *Annual Review of Ecology and Systematics*, *18*(1), 293–320. https://doi.org/10.1146/annurev.es.18.110187.001453

Pradhananga, D., & Pomeroy, J. W. (2022). Recent hydrological response of glaciers in the Canadian Rockies to changing climate and glacier configuration. *Hydrology and Earth System Sciences*, *26*(10), 2605–2616. https://doi.org/10.5194/hess-26-2605-2022

Pucher, M., Wünsch, U., Weigelhofer, G., Murphy, K., Hein, T., & Graeber, D. (2019). staRdom: Versatile Software for Analyzing Spectroscopic Data of Dissolved Organic Matter in R. *Water*, *11*(11), 2366. https://doi.org/10.3390/w11112366

Qiagan. (2019). *Powerwater Sterivex kit manufacturer protocol*.

R Core Team. (2022). R: A language and environment for statistical computing. R Foundation for Statistical Computing, Vienna, Austria. *Online: Https://Www. r-Project. Org*.

Rau, G. H., & Hedges, J. I. (1979). Carbon-13 depletion in a hydrothermal vent mussel: Suggestion of a chemosynthetic food source. *Science (New York, N.Y.)*, *203*(4381), 648–649. https://doi.org/10.1126/science.203.4381.648

Raymond, P. A., & Bauer, J. E. (2001). Use of 14C and 13C natural abundances for evaluating riverine, estuarine, and coastal DOC and POC sources and cycling: A review and synthesis. *Organic Geochemistry*, *32*(4), 469–485. https://doi.org/10.1016/S0146-6380(00)00190-X

Roach, K. A. (2013). Environmental factors affecting incorporation of terrestrial material into large river food webs. *Freshwater Science*, *32*(1), 283–298. https://doi.org/10.1899/12-063.1

Ruby, E. G., Jannasch, H. W., & Deuser, W. G. (1987). Fractionation of Stable Carbon Isotopes during Chemoautotrophic Growth of Sulfur-Oxidizing Bacteria. *Applied and Environmental Microbiology*, *53*(8), 1940–1943.

Shi, Z., Allison, S. D., He, Y., Levine, P. A., Hoyt, A. M., Beem-Miller, J., Zhu, Q., Wieder, W. R., Trumbore, S., & Randerson, J. T. (2020). The age distribution of global soil carbon inferred from radiocarbon measurements. *Nature Geoscience*, *13*(8), Article 8. https://doi.org/10.1038/s41561-020-0596-z

Shutova, Y., Baker, A., Bridgeman, J., & Henderson, R. K. (2014). Spectroscopic characterisation of dissolved organic matter changes in drinking water treatment: From PARAFAC analysis to online monitoring wavelengths. *Water Research*, *54*, 159–169. https://doi.org/10.1016/j.watres.2014.01.053

Singer, G. A., Fasching, C., Wilhelm, L., Niggemann, J., Steier, P., Dittmar, T., & Battin, T. J. (2012). Biogeochemically diverse organic matter in Alpine glaciers and its downstream fate. *Nature Geoscience*, *5*(10), Article 10. https://doi.org/10.1038/ngeo1581

Smith, B. P. G., Hannah, D. M., Gurnell, A. M., & Petts, G. E. (2001). A hydrogeomorphological context for ecological research on alpine glacial rivers. *Freshwater Biology*, *46*(12), 1579–1596. https://doi.org/10.1046/j.1365-2427.2001.00846.x

Smith, H. J., Foster, R. A., McKnight, D. M., Lisle, J. T., Littmann, S., Kuypers, M. M. M., & Foreman, C. M. (2017). Microbial formation of labile organic carbon in Antarctic glacial environments. *Nature Geoscience*, *10*(5), 356–359. https://doi.org/10.1038/ngeo2925

Spencer, R. G. M., Guo, W., Raymond, P. A., Dittmar, T., Hood, E., Fellman, J., & Stubbins, A. (2014). Source and biolability of ancient dissolved organic matter in glacier and lake ecosystems on the Tibetan Plateau. *Geochimica et Cosmochimica Acta*, *142*, 64–74. https://doi.org/10.1016/j.gca.2014.08.006

Spencer, S. A., Anderson, A. E., Silins, U., & Collins, A. L. (2021). Hillslope and groundwater contributions to streamflow in a Rocky Mountain watershed underlain by glacial till and fractured sedimentary bedrock. *Hydrology and Earth System Sciences*, *25*(1), 237–255. https://doi.org/10.5194/hess-25-237-2021

Stedmon, C. A., & Markager, S. (2005). Resolving the variability in dissolved organic matter fluorescence in a temperate estuary and its catchment using PARAFAC analysis. *Limnology and Oceanography*, *50*(2), 686–697. https://doi.org/10.4319/lo.2005.50.2.0686

Stevens, I. T., Irvine-Fynn, T. D. L., Edwards, A., Mitchell, A. C., Cook, J. M., Porter, P. R., Holt, T. O., Huss, M., Fettweis, X., Moorman, B. J., Sattler, B., & Hodson, A. J. (2022). Spatially consistent microbial biomass and future cellular carbon release from melting Northern Hemisphere glacier surfaces. *Communications Earth & Environment*, *3*(1), Article 1. https://doi.org/10.1038/s43247-022-00609-0

Stibal, M., Šabacká, M., & Žárský, J. (2012a). Biological processes on glacier and ice sheet surfaces. *Nature Geoscience*. https://doi.org/10.1038/ngeo1611

Stubbins, A., Hood, E., Raymond, P. A., Aiken, G. R., Sleighter, R. L., Hernes, P. J., Butman, D., Hatcher, P. G., Striegl, R. G., Schuster, P., Abdulla, H. A. N., Vermilyea, A. W., Scott, D. T., & Spencer, R. G. M. (2012a). Anthropogenic aerosols as a source of ancient dissolved organic matter in glaciers. *Nature Geoscience*, *5*(3), 198–201. https://doi.org/10.1038/ngeo1403

Tamames, J., Abellán, J. J., Pignatelli, M., Camacho, A., & Moya, A. (2010). Environmental distribution of prokaryotic taxa. *BMC Microbiology*, *10*(1), 85. https://doi.org/10.1186/1471-2180-10-85

Teske, A., & Salman, V. (2014). The Family Beggiatoaceae. In E. Rosenberg, E. F. DeLong, S. Lory, E. Stackebrandt, & F. Thompson (Eds.), *The Prokaryotes* (pp. 93–134). Springer Berlin Heidelberg. https://doi.org/10.1007/978-3-642-38922-1_290

Tonkin, J. D., Altermatt, F., Finn, D. S., Heino, J., Olden, J. D., Pauls, S. U., & Lytle, David. A. (2018). The role of dispersal in river network metacommunities: Patterns, processes, and pathways. *Freshwater Biology*, *63*(1), 141–163. https://doi.org/10.1111/fwb.13037

Tranter, M., Sharp, M. J., Lamb, H. R., Brown, G. H., Hubbard, B. P., & Willis, I. C. (2002). Geochemical weathering at the bed of Haut Glacier d'Arolla, Switzerland—A new model. *Hydrological Processes*, *16*(5), 959–993. https://doi.org/10.1002/hyp.309

Wadham, J. L., Hawkings, J. R., Tarasov, L., Gregoire, L. J., Spencer, R. G. M., Gutjahr, M., Ridgwell, A., & Kohfeld, K. E. (2019). Ice sheets matter for the global carbon cycle. *Nature Communications*, *10*(1). https://doi.org/10.1038/s41467-019-11394-4

Weishaar, J. L., Aiken, G. R., Bergamaschi, B. A., Fram, M. S., Fujii, R., & Mopper, K. (2003). Evaluation of Specific Ultraviolet Absorbance as an Indicator of the Chemical Composition and Reactivity of Dissolved Organic Carbon. *Environmental Science & Technology*, *37*(20), 4702–4708. https://doi.org/10.1021/es030360x

Whiteside, J. H., Olsen, P. E., Eglinton, T. I., Cornet, B., McDonald, N. G., & Huber, P. (2011). Pangean great lake paleoecology on the cusp of the end-Triassic extinction. *Palaeogeography, Palaeoclimatology, Palaeoecology*, *301*(1), 1–17. https://doi.org/10.1016/j.palaeo.2010.11.025

Wickham H. (2016). *ggplot2: Elegant Graphics for Data Visualization*. https://ggplot2.tidyverse.org/

Wilhelm, L., Singer, G. A., Fasching, C., Battin, T. J., & Besemer, K. (2013). Microbial biodiversity in glacier-fed streams. *The ISME Journal*, *7*(8), Article 8. https://doi.org/10.1038/ismej.2013.44

Zeglin, L. H. (2015). Stream microbial diversity in response to environmental changes: Review and synthesis of existing research. *Frontiers in Microbiology*, *6*. https://www.frontiersin.org/articles/10.3389/fmicb.2015.00454

Zemp, M., Frey, H., Gärtner-Roer, I., Nussbaumer, S. U., Hoelzle, M., Paul, F., Haeberli, W., Denzinger, F., Ahlstrøm, A. P., Anderson, B., Bajracharya, S., Baroni, C., Braun, L. N., Cáceres, B. E., Casassa, G., Cobos, G., Dávila, L. R., Granados, H. D., Demuth, M. N.,

… Vincent, C. (2015). Historically unprecedented global glacier decline in the early 21st century. *Journal of Glaciology*, *61*(228), 745–762. https://doi.org/10.3189/2015JoG15J017

Zhang, Y., Kang, S., Li, G., Gao, T., Chen, P., Li, X., Liu, Y., Hu, Z., Sun, S., Guo, J., Wang, K., Chen, X., & Sillanpää, M. (2018). Dissolved organic carbon in glaciers of the southeastern Tibetan Plateau: Insights into concentrations and possible sources. *PLOS ONE*, *13*(10), e0205414. https://doi.org/10.1371/journal.pone.0205414

Zheng, Q., Lu, J., Wang, Y., & Jiao, N. (2019). Genomic reconstructions and potential metabolic strategies of generalist and specialist heterotrophic bacteria associated with an estuary Synechococcus culture. *FEMS Microbiology Ecology*, *95*(3), fiz017. https://doi.org/10.1093/femsec/fiz017

Zhou, Y., Zhou, L., He, X., Jang, K.-S., Yao, X., Hu, Y., Zhang, Y., Li, X., Spencer, R. G. M., Brookes, J. D., & Jeppesen, E. (2019). Variability in Dissolved Organic Matter Composition and Biolability across Gradients of Glacial Coverage and Distance from Glacial Terminus on the Tibetan Plateau. *Environmental Science & Technology*, *53*(21), 12207–12217. https://doi.org/10.1021/acs.est.9b03348

Appendix

A.1: Site characteristics

Distance Range	Glacier headwaters	River	Latitude	Longitude	Distance from glacier terminus (km)	Number of times visited
Far	Athabasca	Athabasca	52°34' 59.6"	-117°44'21.9"	50	14
Far	Athabasca	Athabasca	52°39′46.5”	-117°52′51.7"	70	18
Far	Athabasca	Athabasca	52°48′43.4"	-118°02′33.2"	100	16
Headwater	Athabasca	Sunwapta	52°12'25.8"	-117°14'05.9"	0	16
Near	Athabasca	Sunwapta	52°12'59.5"	-117°14'01.9"	3	15
Mid	Athabasca	Sunwapta	52°18′38.1"	-117°19′57.3"	25	17
Far	Athabasca	Sunwapta	52°31′58.7"	-117°38′39.2"	50	17
Near	Saskatchewan	NSR	52°10′10.1"	-117°04′34.9"	7	18
Mid	Saskatchewan	NSR	52°4'9.1"	-116°54'54.9"	18	16
Far	Saskatchewan	NSR	51°58′14.0"	-116°43′16.0"	35	16
Near	Bow	Bow	51°39'42.3"	-116°29'12.98"	2	14
Mid	Bow	Bow	51°37'53.04"	-116°20'6.6"	15	15
Mid	Bow	Bow	51°25′43.2"	-116°11′20.4"	40	17

Table A.2: End member isotope values from Ardent (2015) utilized in a water isotope mixing model.

End Member	$\delta^{18}O$	d excess
Glacier ice	-20.0	20
Snow	-25.5	-1
Summer precipitation	-13.0	0

Table A.3. Excitation and emission maxima associated with PARAFAC components and associated DOM character as assessed by cross reference with the Open Fluor database.

Component	Emission peak	Excitation peak	Character	Number of Open Fluor Matches
C1	271	230	Terrestrial / humic (Shutova et al., 2014)	118
C2	409	230	Terrestrial / humic (Catalán et al., 2018; Coulson et al., 2022; Shutova et al., 2014),	105
C3	340	230	Microbial/tryptophan like (Murphy et al., 2008; Stedmon & Markager, 2005)	27
C4	300	230, 270-275	Microbial/tyrosine like(Graeber et al., 2012)	14

Table A.4. Description of characteristics for various the absorbance- and fluorescence-based metrics used in this study.

Measurement	Calculation	Purpose
$SUVA_{254}$	Normalization of UV absorbance at 254 nm to DOC	Increasing values indicate increasing aromaticity (Weishaar et al. 2003)
$S_{275\text{-}295}$	Slope over the 275nm-295nm wavelength range	Decreasing values indicates increasing molecular weight (Helms et al. 2008)
BIX	The ratio of emission at 380nm by 430nm at excitation of 310nm	Biological Index: Increasing values indicate recently produced organic carbon (Huguet et al. 2008)
HIX	Fluorescence intensity over 300-340nm divided by the combined fluorescence in the 300-345nm and 435-480nm	Humification Index; Increasing values indicate increasing humification (Ohno 2002)
FI	The ratio of emission at 400nm to 500nm at an excitation of 370nm	Fluorescence Index: Higher values indicate microbially derived fulvic acids, lower values indicate terrestrially derived fulvic acids (McKnight et al. 2001)

Table A.5. Outputs from a two-way ANOVA to show the effect of distance range and hydrological season on the relative percentage of glacial ice in stream water. Interaction effects and Tukey's HSD comparisons for main effects are also shown. Significant main effects and post-hoc comparisons are bolded.

Glacier ice						
Factor	**Df**	**SumSq**	**F value**	**p**	**Tukey Comparison**	**p**
Distance Range	3	2133	41.116	**< 0.0001**	Headwater=Near	0.11
					Headwater>Mid	**<0.0001**
					Headwater>Far	**<0.0001**
					Near>Mid	**0.0001**
					Near>Far	**<0.0001**
					Mid>Far	**<0.0001**
Season	2	326	9.424	**0.0001**	PreMelt<Melt	**<0.0001**
					PreMelt=PostMelt	0.065
					Melt=PostMelt	0.36
DistRange: Season	6	146	1.403	0.22		
Residuals	186	3217				

Table A.6. Outputs from a two-way ANOVA to show the effect of distance range and hydrological season on the relative percentage of summer precipitation in stream water. Interaction effects and Tukey's HSD comparisons for main effects are also shown. Significant main effects and post-hoc comparisons are bolded.

Summer precipitation						
Factor	**Df**	**SumSq**	**F value**	**p**	**Tukey Comparison**	**p**
Distance Range	3	2133	41.116	**< 0.0001**	Headwater=Near	0.11
					Headwater>Mid	**<0.0001**
					Headwater>Far	**<0.0001**
					Near>Mid	**0.0001**
					Near>Far	**<0.0001**
					Mid>Far	**<0.0001**
Season	2	326	9.424	**0.0001**	PreMelt<Melt	**<0.0001**
					PreMelt=PostMelt	0.065
					Melt=PostMelt	0.36
DistRange: Season	6	146	1.403	0.22		
Residuals	186	3217				

Table A.7 Outputs from a three-way ANOVA to show the effect of distance range, hydrological season, and year on the DOC concentration in stream water. Interaction effects and Tukey's HSD comparisons for main effects are also shown. Significant main effects and post-hoc comparisons are bolded.

DOC						
Factor	**Df**	**SumSq**	**F value**	**p value**	**Tukey Comparison**	**p**
Distance Range	3	8.531	26.983	**<0.0001**	Headwater = Near	0.99
					Headwater = Mid	0.081
					Headwater < Far	**<0.0001**
					Near < Mid	**0.0034**
					Near < Far	**<0.0001**
					Mid < Far	**<0.0001**
Hydrological Season	1	5.488	52.074	**<0.0001**	PreMelt > Melt	**<0.0001**
Year	2	0.997	4.731	0.0102	2019>2020	**0.033**
					2019>2021	**0.014**
					2020=2021	0.93
DistRange: Season	3	1.365	4.318	0.006		
DistRange: Year	6	1.431	2.263	0.041		
Season: Year	1	3.480	33.025	**<0.0001**		
DistRange: Season:Year	3	1.344	4.25113	0.007		
Residuals	152	15.492	NA	NA		

Table A.8 Outputs from a three-way ANOVA to show the effect of distance range, hydrological season, and year on the POC concentration in stream water. Interaction effects and Tukey's HSD comparisons for main effects are also shown. Significant main effects and post-hoc comparisons are bolded.

POC						
Factor	**Df**	**SumSq**	**F value**	**P value**	**Tukey Comparison**	**p**
Distance Range	3	1.746	3.281	**0.023**	Headwater > Near	**0.019**
					Headwater = Mid	0.31
					Headwater = Far	0.077
					Near = Mid	0.23
					Near = Far	0.69
					Mid = Far	0.72
Hydrological Season	1	0.240	1.352	0.246		
Year	2	1.110	3.129	**0.046**	2019=2020	0.67
					2019>2021	**0.05**
					2020=2021	0.21
DistRange: Season	3	0.390	0.463	0.71		
DistRange: Year	6	1.649	1.550	0.166		
Season: Year	1	0.01	0.056	0.813		
DistRange: Season:Year	3	0.0431	0.081	0.970		
Residuals	149	26.425	NA	NA		

Table A.9. Outputs from a three-way ANOVA to show the effect of distance range, hydrological season, and year on the relative proportion of protein-like DOM in stream water. Interaction effects and Tukey's HSD comparisons for main effects are also shown. Significant main effects and post-hoc comparisons are bolded.

Protein-like components						
Factor	**Df**	**SumSq**	**F value**	**P value**	**Tukey Comparison**	**p**
Distance Range	3	3.215	29.183	**<0.0001**	Headwater > Near	0.21
					Headwater > Mid	**<0.0001**
					Headwater > Far	**<0.0001**
					Near > Mid	**<0.0001**
					Near > Far	**<0.0001**
					Mid > Far	**0.025**
Season	1	0.357	9.729	**0.00216**	PreMelt - Melt	**0.002**
Year	2	0.236	3.216	**0.043**	2019=2020	0.12
					2019=2021	0.071
					2020=2021	0.95
DistRange: Season	3	0.057	0.518	0.67		
DistRange: Year	6	0.423	1.922	**0.08**		
Season: Year	1	0.001	0.016	0.9		
DistRange: Season:Year	3	0.077	0.701	0.55		
Residuals	158	5.802				

Table A.10. Outputs from a three-way ANOVA to show the effect of distance range, hydrological season, and year on δ^{13}C-DOC ‰ in stream water. Interaction effects and Tukey's HSD comparisons for main effects are also shown. Significant main effects and post-hoc comparisons are bolded.

δ^{13}C-DOC						
Factor	**Df**	**SumSq**	**F value**	**p**	**Tukey comparison**	**p**
Distance Range	3	11.2	1.014	0.39		
Season	2	45	6.088	**0.003**	PreMelt=Melt	0.12
					PreMelt<PostMelt	**0.003**
					Melt<PostMelt	**0.03**
Year	2	225	30.455	**<0.0001**	2019>2020	**<0.0001**
					2019>2021	**<0.0001**
					2020=2021	0.45
DistRange: Season	6	86.8	3.916	**0.0014**		
DistRange: Year	6	115.2	5.197	**<0.0001**		
Season: Year	2	46.1	6.245	**0.0027**		
DistRange: Season:Year	3	5.1	0.459	0.71		
Residuals	115	424.9				

Table A.11. Outputs from a three-way ANOVA to show the effect of distance range, hydrological season, and year on δ^{13}C-POC **‰** in stream water. Interaction effects and Tukey's HSD comparisons for main effects are also shown. Significant main effects and post-hoc comparisons are bolded.

δ^{13}C-POC						
Factor	**Df**	**SumSq**	**F value**	**p**	**Tukey Comparison**	**p**
Distance Range	3	14.5	1.743	0.16		
Season	2	69.8	12.604	**<0.0001**	PreMelt<Melt	**<0.001**
					PreMelt<PostMelt	**0.002**
					Melt=PostMelt	0.93
Year	2	489.4	88.35	**<0.001**	2019<2020	**<0.001**
					2019<2021	**<0.001**
					2020=2021	0.19
DistRange: Season	6	35.2	2.118	**0.05**		
DistRange: Year	6	52.2	3.139	**0.006**		
Season: Year	3	6.1	0.732	0.53		
DistRange: Season:Year	7	37.2	1.92	**0.07**		**.**
Residuals	146	404.4				

Table A.12. Outputs from a two-way ANOVA to show the effect of distance range and hydrological season on Δ^{14}C-DOC **‰** in stream water. Interaction effects and Tukey's HSD comparisons for main effects are also shown. Significant main effects and post-hoc comparisons are bolded.

Δ^{14}C-DOC						
Factor	**Df**	**SumSq**	**F value**	**p**	**Tukey comparison**	**p**
Distance Range	3	142056	2.37	0.085		
Season	2	269461	6.743	**0.003**	PreMelt = melt	0.47
					PreMelt > postmelt	**0.0044**
					melt > PostMelt	**0.011**
DistRange: Season	3	5032	0.084	0.97		
Residuals	40	799220				

Table A.13. PERMANOVA test outputs showing the variation between proportion of microbial-communities by distance range, hydrological season, year, and river. PERMANOVA pairwise comparisons with holm adjusted p values are shown. Significant interactions are bolded.

Factor	R^2	significance	PERMANOVA pairwise comparison	p (holm adjusted)
Distance Range	0.09	< 0.001	Headwater - Near	0.1659
			Headwater - Far	**0.0044**
			Near - Far	**0.0003**
Year	0.08	<0.001	2019-2020	**0.0003**
			2019-2021	**0.0024**
			2020-2021	**0.0068**
Season	0.06	0.002	PreMelt – Melt	**0.0039**
			PreMelt – PostMelt	0.0602
			Melt – PostMelt	0.2125
River	0.08	<0.001	Sunwapta-Athabasca	**0.0027**
			Sunwapta-NSR	**0.0003**
			Athabasca-NSR	**0.0003**

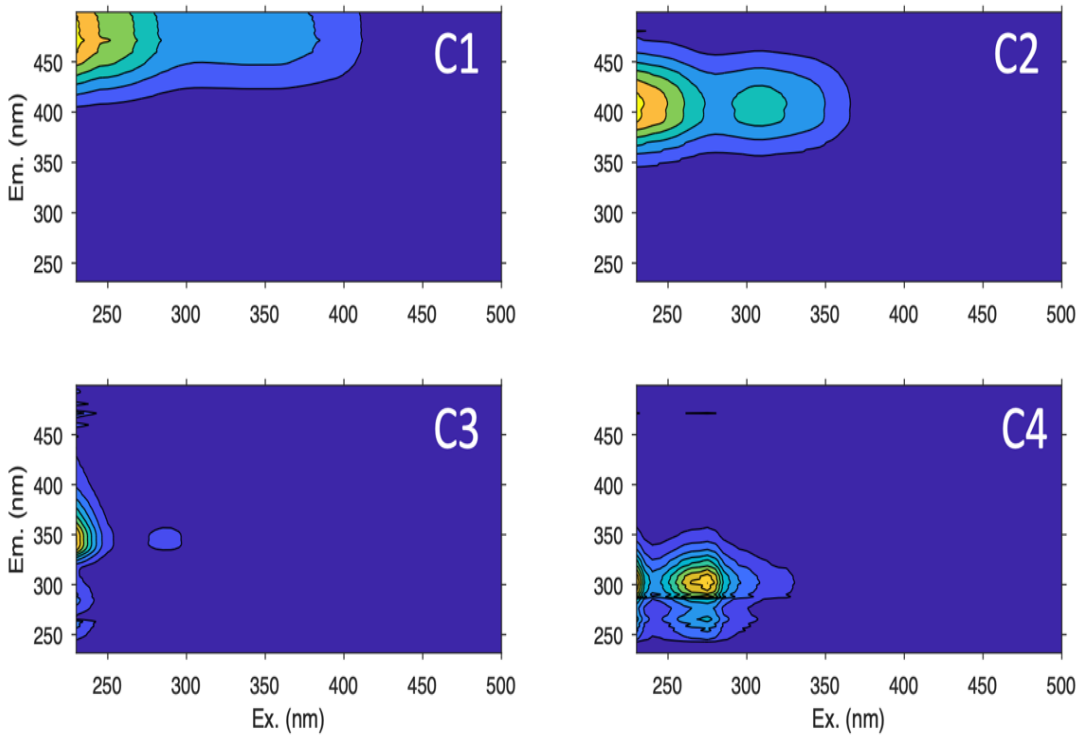

Figure A.1. Component plots for the four-component PARAFAC model

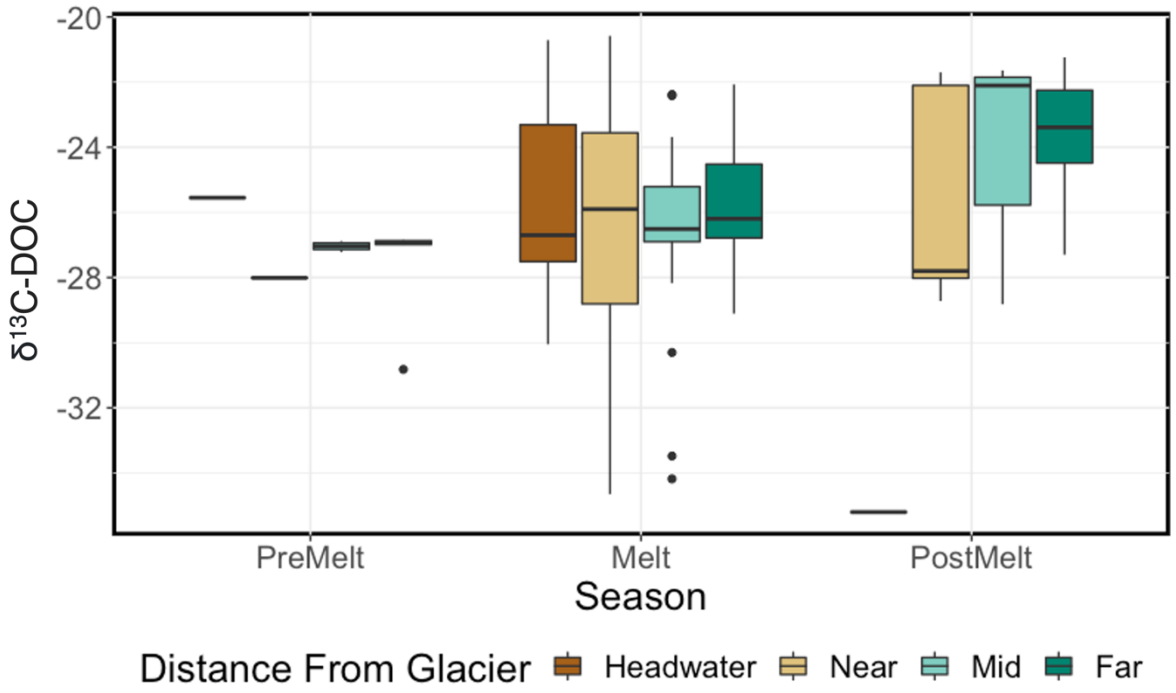

Figure A.2 Boxplot of stream δ^{13}C-DOC values for pre-melt, melt and post-melt hydrological periods grouped by distance range. The boxes represent the interquartile range, the black line represents the median value, and the points represent outliers.

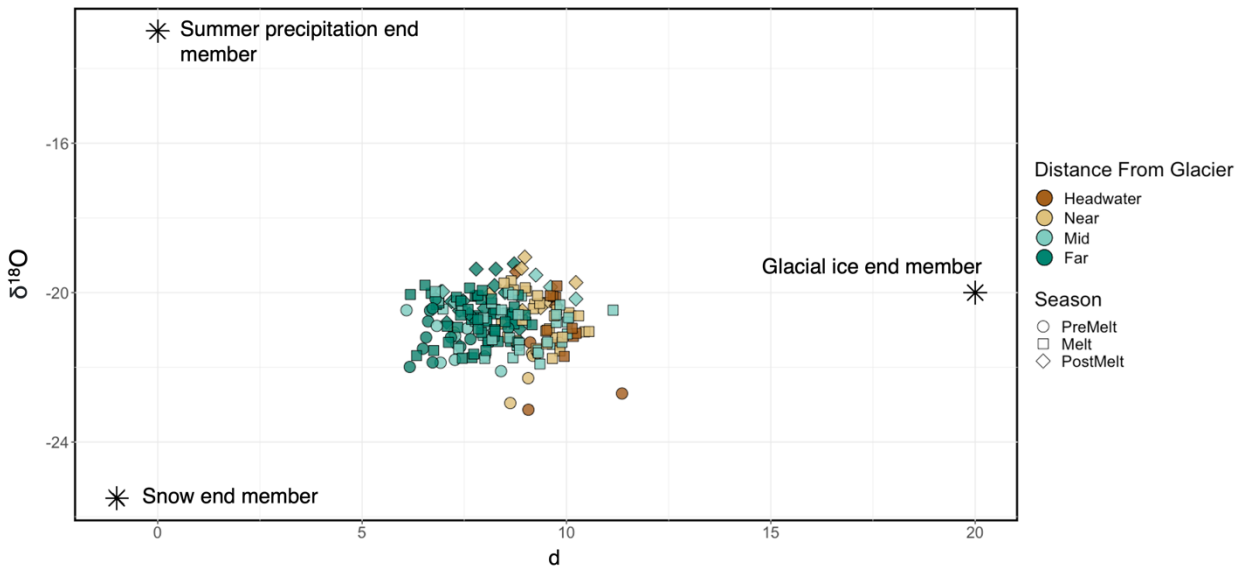

Figure A.3 $\delta^{18}O$-H_2O versus d for stream water samples with end member values for glacial ice, snow and summer precipitation from the Athabasca glacier in 2011 (Arendt, 2015).

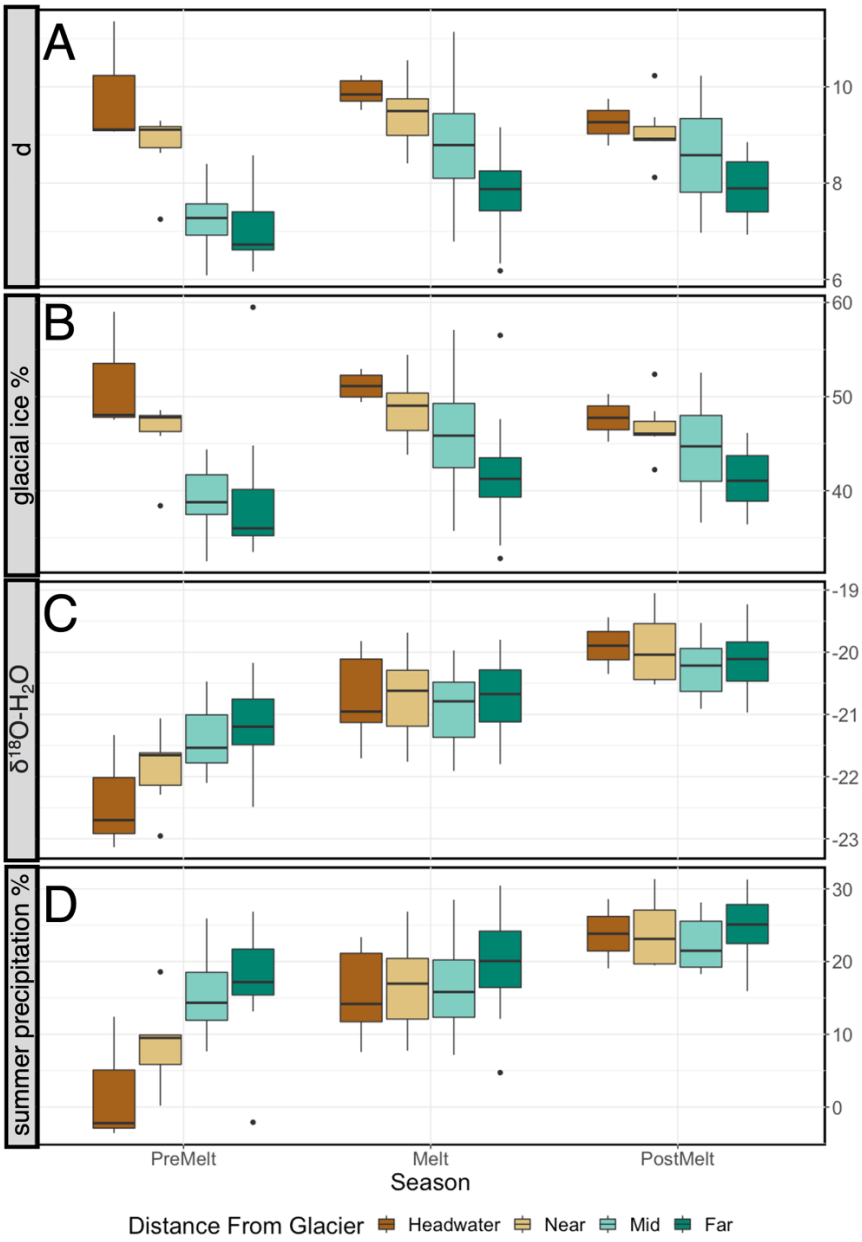

Figure A.4. Boxplots of (A) deuterium excess (d), (B) glacial ice (%) (C) $\delta^{18}O$-H_2O, and (D) relative percentage of summer precipitation within streams across pre-melt, melt and post-melt hydrological periods grouped by distance range downstream from glacial terminus. The boxes represent the interquartile range, the black line represents the median value, and the points represent outliers.

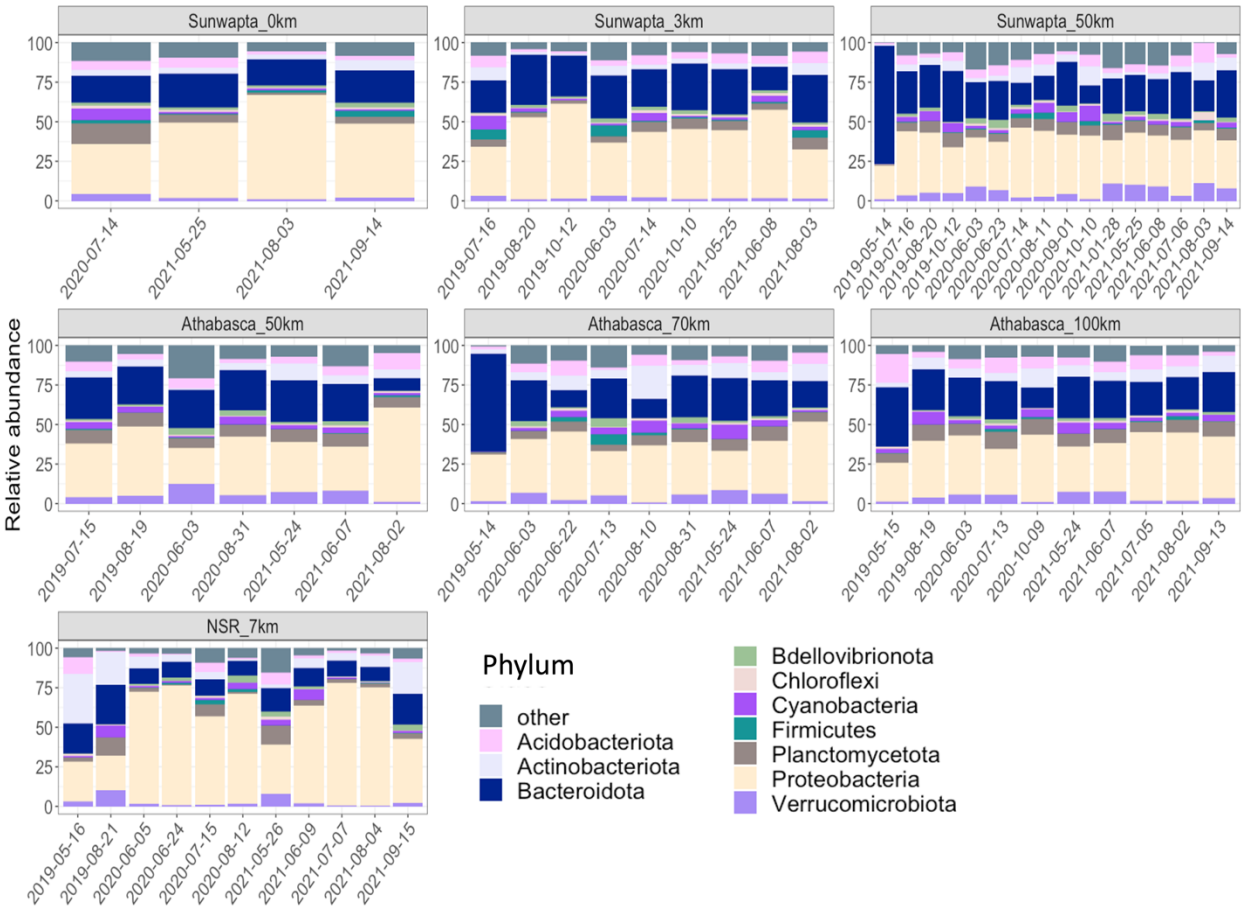

Figure A.5: Relative abundance of the top ten most abundant taxonomic phyla across all sites and sampling dates. The category "Other" represents classes not included in the top ten.

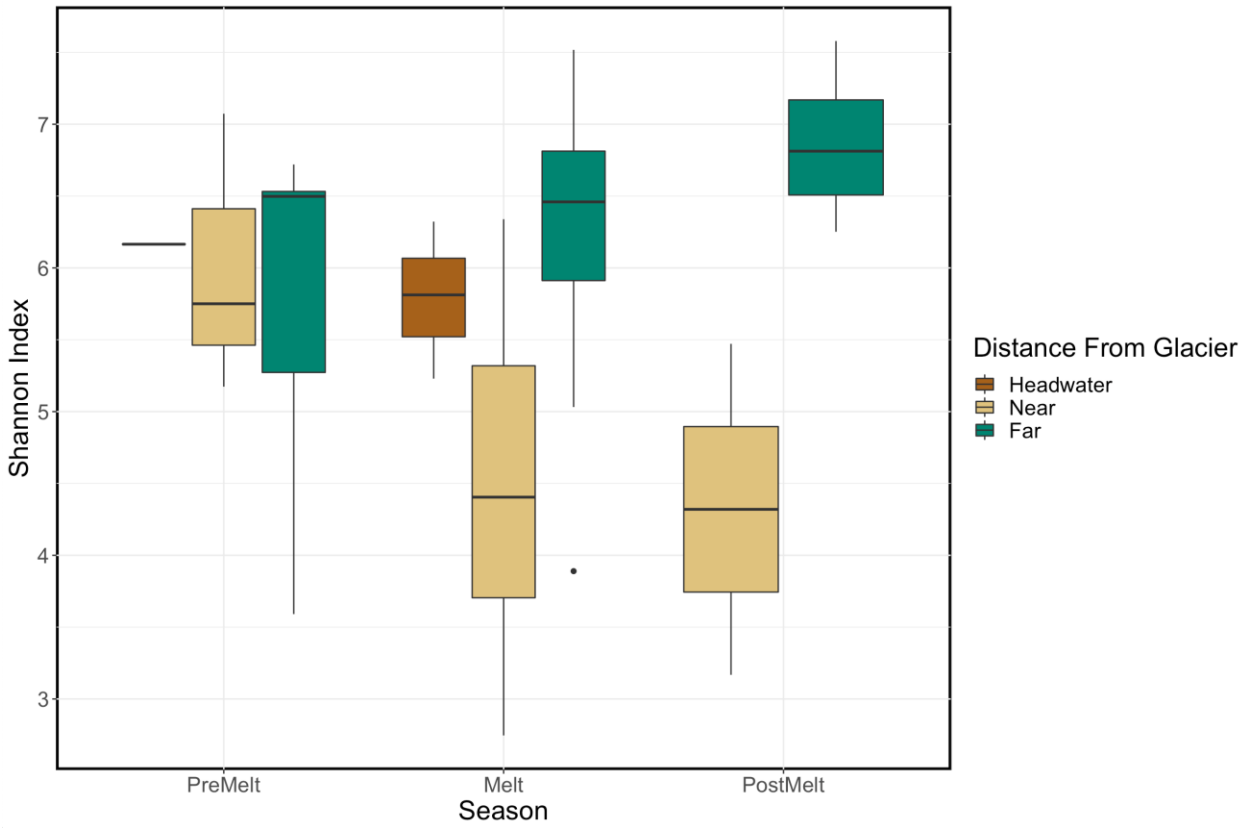

Figure A.6: Boxplots to show variation in alpha diversity across hydrological periods and distance range, using the Shannon diversity index. The boxes represent the interquartile range, the black line represents the median value, and the points represent outliers.

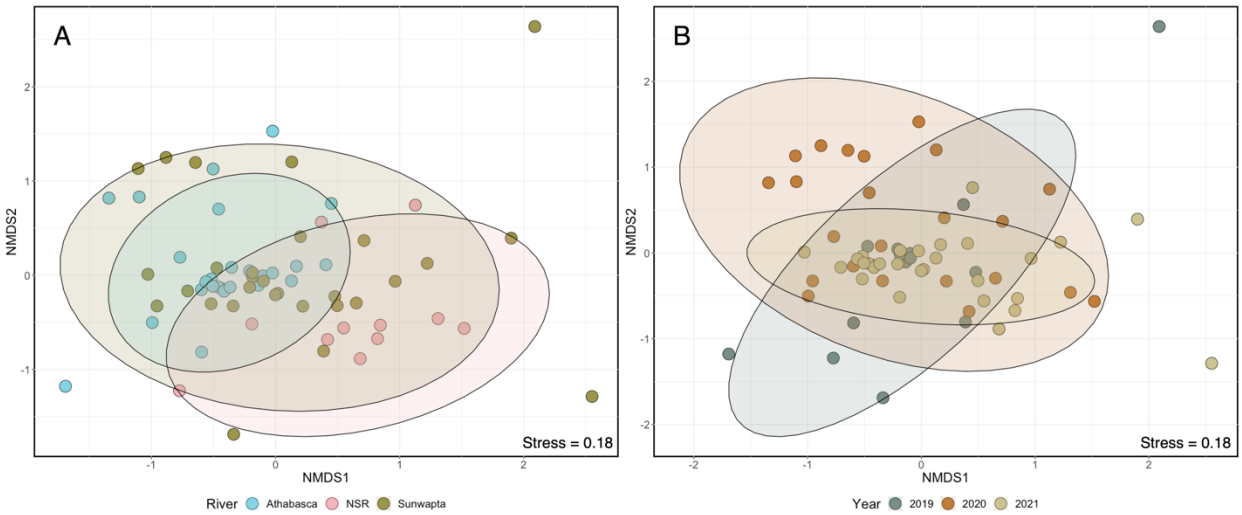

Figure A.7: NMDS of microbial community composition based on Bray Curtis distances of Hellinger transformed ASV data. Colour represents different (A) study rivers and (B) sampling years. Shaded circles represent the 95% confidence interval for significantly different groupings (pairwise permanova $p < 0.01$ (holms adjusted) see Table. A.13).